

# Reviewer 1

We thank the reviewer for all their helpful critiques and suggestions that helped us improve this manuscript. Reviewer comments are given in black. Our responses are given in red, and the updated text in this document is blue.

The authors examine warm rain efficiency (WRE) in marine liquid clouds using rain water path estimates from the CloudSat Cloud Profiling Radar and cloud water path from MODIS. They show that WRE increases as cloud extent increases after controlling for cloud top height and low level relative humidity. AOD shows little correlation with WRE when conditioned by cloud top height indicating potentially limited aerosol impacts on WRE once warm rain has begun. WRE increases as expected with SST due to clouds that are deeper with more condensed water but this study also shows that WRE also increases with cloud extent for a given SST and cloud extents grow with SST. Thus, increased WRE as SST increases could also partly result from larger clouds that are more protected from dry air entrainment.

I can somewhat buy into the primary argument of this study that larger clouds are more protected from deleterious dry air entrainment and thus are more apt to form rain. However, there are a number of additional considerations that have to be discussed before such a conclusion can be reached, highlighted in the major comments below. In Addition, some plots and methods used need improvement, again highlighted in more detail below.

## Major Comments

1. The title indicates that “warm rain likelihood” is examined in addition to warm rain efficiency but nearly the entire study focuses on warm rain efficiency and does not consider clouds that are not already raining. Thus, I recommend changing the title of the paper.
  - a. **The title has been updated to “A-Train estimates of the sensitivity of the cloud to rain water ratio to cloud size, relative humidity, and aerosols”.**
2. The clouds being analyzed in this study are repeatedly referred to as shallow cumulus clouds but the cloud length scales examined are 1.7 to 18 km, so this is combining quite robust cumulus clouds at the short end of the spectrum with wider presumably stratocumulus clouds at the longer end of the spectrum. This makes the “shallow cumulus” terminology misleading for me. Applying a simple 18.55 K lower tropospheric stability separator will not filter out all stratocumulus clouds. In addition, many shallow cumulus are smaller than the CloudSat CPR footprint of 1.8 x 1.4 km, so the clouds at this end of the spectrum will suffer from non-uniform beam filling that can bias retrievals (e.g., Battaglia et al. 2020).
  - a. **The 18.55K LTS threshold has been commonly used in the literature as a robust separator between the two regimes (Klein and Hartmann, 1993). However, to further examine the possible influence of stratocumulus on our results, we re-ran the analysis for both the global oceans, excluding the southeast Pacific, northeast Pacific, southeast Atlantic, northeast Atlantic, and Indian ocean stratocumulus region. We also separately analyzed only the south Pacific trade cumulus region (excluding the southeast Pacific stratocumulus region). Our overall results and their interpretation do not change if we only analyze regions of mostly shallow cumulus. This lends credibility to LTS being an effective separator between shallow and stratocumulus, and that the majority of cloud objects we identify are shallow cumulus. However, given this may be a concern that future readers might have, we have added the following text (Pages 9-10, Lines 288-294) to the paper : “It is surprising that this study identifies shallow cumulus cloud objects larger than 10 km. This suggests that some stratocumulus are not being filtered out of this dataset by our LTS threshold. However, a majority of cloud objects that we identify have extents below 10 km. This is consistent with Figure 1e which shows that a majority of cloud objects occur over regions generally associated with shallow cumulus. To further test this, we performed the same analysis over the south pacific**

*trade region but excluded the southeast stratocumulus region, and we still find few large cloud objects with our overall results not changing. This suggests that predominant type of entrainment impacting these cloud objects would be lateral entrainment at cloud edges (see review by de Rooy et al., 2013), and that these are indeed shallow cumulus.”.*

- b.** *With regards to your second point that there are likely shallow cumulus smaller than the CloudSat footprint, unfortunately this is unavoidable given CloudSat’s resolution. We had discussed the potential impacts of beam filling and clouds below the satellite FOV side in our previous paper (Smalley and Rapp, 2020) that this one is a follow-on to, but did not repeat the discussion here. However, to address issues related to resolution and cloud scales, we have added the following text (Page 10, Lines 295-299) to the paper: “At the small end of the shallow cumulus horizontal size spectrum, CloudSat is limited to observing cloud objects no smaller than 1.4 x 1.8 km. Given prior ground observational studies, it is likely that there is a significant population of shallow cumulus cloud objects not identified by our study (e.g. Kollias et al., 2003; Mieslinger et al., 2019) due to non-uniform beam filling effects. Battaglia et al. (2020) noted that this results in an underestimation of path integrated attenuation, potentially introducing error into the retrieval of  $W_p$ . Unfortunately, this limitation is unavoidable given CloudSat’s horizontal resolution.”.*

3. The assumption that clouds are shallow cumulus feeds into the assumption that lateral entrainment is the key process controlling WRE, which is stated repeatedly throughout the study. Lateral entrainment is important for km-scale cumulus clouds but cloud top entrainment is important for 10s of kilometers scale stratocumulus clouds. In addition, is there anything to suggest that once a relatively shallow liquid cloud is wider than multiple kilometers that its core is not protected from lateral entrainment? There are too many assumptions being made regarding the importance of entrainment without supporting evidence. Another potentially major contributor to warm rain efficiency that also correlates with cloud size is cloud lifetime, which should be discussed but isn't. Larger clouds typically live longer, which could increase the probability of rain formation. Other factors that could impact WRE that are not mentioned but should be include turbulent enhancement of droplet collision-coalescence, updraft speed controls on the supersaturation and number of droplets condensed, and potential time lags between peaks in rain water path and cloud water path due to raindrops consuming cloud droplets.

**a. As described in major comment 2, we believe that we are sampling predominantly shallow cumulus. Excluding regions of the globe where stratocumulus are common does not change our overall findings. As to your other concerns regarding other possible factors contributing to changes in warm rain efficiency, we agree that there are potential processes other than entrainment which may contribute to higher warm rain efficiency with cloud size, and they are now described in the following text (Page 9, Lines 268-287):** *“This study has emphasized the potential for the decreasing impact of entrainment on cloud cores, resulting in higher WRR, as cloud size increases; however, it is important to point out other factors related to cloud size that may also impact WRR. Figure 3 shows WRR is higher when cloud objects are taller, which may be simply because we are sampling more mature clouds that have had more time for the collision-coalescence process to result in rain formation. Deeper shallow cumulus not only live longer which would give cloud droplets more time to grow to raindrop size (e.g. Burnet and Brenguier, 2010), but they are more likely to have more intense updrafts which could result in more water vapor being transported to higher altitudes within a cloud. Stronger updrafts are then more likely to be able to suspend cloud droplets higher in the cloud for longer periods of time which allows them to grow larger before they begin to fall and collision-coalescence is initiated. Once cloud droplets do begin to fall, they are not only potentially larger but able*

*to collect more droplets over a larger distance than droplets falling through a shallower cloud. This could potentially result in higher WRR, however there is likely a lag between the peaks in cloud water path and rain water path as cloud drops grow to raindrop size in a developing cloud. Earlier modeling studies have also noted that turbulent flow potentially enhances the likelihood of warm rain formation (e.g. Brenguier and Chaumat, 2001; Seifert et al., 2010; Wyszogrodzki et al., 2013; Franklin, 2014; Seifert and Onishi, 2016; Chen et al., 2018). Seifert et al. (2010) found that turbulence effects are largest near cloud tops in shallow cumulus, which they note is an important region for initial rain formation. While these additional processes may impact WRR, the satellite observations used in this study are instantaneous snapshots in time. We attempted to remove some of these life cycle impacts by binning cloud objects by top height. Within a given cloud top height bin, WRR (Figure 3) and the magnitude of  $VGZ_{CP}$  (Figure 4c) still increase as a function of extent. While we acknowledge that this cannot fully remove these impacts, these results support the idea that processes other than those related to cloud lifetime, like lateral entrainment, may also influence the WRR of shallow cumulus of different horizontal sizes”.*

4. Lines 67-68: It is made to seem like there are very few studies examining relationships between cloud water and precipitation in shallow cumulus as a function of cloudsize, moisture, or aerosol conditions, but this isn't true, and I encourage a more thorough literature review. For example, consider the many studies that have been published using Dominica Experiment (DOMEX) field campaign data. A number of field campaigns and modeling studies have focused on entrainment and precipitation formation of cumulus clouds over land and ocean, and even more have examined stratocumulus clouds.
  - a. **In reference to the sentence that you highlight, we have added more citations in support of those features being looked at primarily using cloud models and field-campaign observations. Please see the following additions to the text (Page 3, Lines 75-79):** *“However, the relationship between cloud water and precipitation as shallow cumulus grow larger, environmental moisture increases, and/or as aerosol loading varies has only been investigated using cloud models (e.g. Abel and Shipway, 2007; vanZanten et al., 2011; Franklin, 2014; Saleeby et al., 2015; Moser and Lasher-Trapp, 2017; Hoffmann et al., 2017) and limited field-campaign observations (e.g. Rauber et al., 2007; Gerber et al., 2008; Burnet and Brenguier, 2010; Watson et al., 2015; Jung et al., 2016b).”*
5. The methodology could use some improvements and clarifications.
  - a. Line 80: The CloudSat CPR cannot always observe non-raining cloud drops because its sensitivity is limited, which has been proven with comparisons to ground sensors (Lamer et al. 2020). In addition, it has ground clutter issues below 1-km altitude. These are important caveats that should be mentioned that could bias sampling.
  - b. What are the uncertainties of the rain water path and cloud water path estimates? On line 92, it indicates that any rain water paths greater than 0 are considered but there should be a minimum value used that is equal to the retrieval uncertainty. For example, for cloud water path, this is typically ~20 g m<sup>-2</sup>.
  - c. Lines 122-123: Average relative humidity below 3 km is a very strange metric for environmental moisture when most of these shallow clouds are interacting with a variable altitude inversion layer. This metric would mix boundary layer air with typically much drier free tropospheric air, which would be weighted by the inversion altitude (which increases as one moves from stratocumulus to trade cumulus regions). The relevant moisture metric for lateral or cloud-top entrainment would be the relative humidity in the lower free troposphere.

- a. The cloud mask threshold of greater than or equal to 20 from 2B-GEOPROF was chosen because it confidently removes CloudSat pixels that may be influenced by ground clutter. We describe this on Page 4, Lines 94-95, *“Contiguous cloudy regions are initially identified using the 2B-GEOPROF (Marchand et al., 2008) cloud mask confidence values  $\geq 20$ , which removes orbit elements that may be influenced by ground clutter (Marchand et al., 2008).”*. **Additionally, the following clarification** *“An additional limitation of CloudSat is its inability to sense the smallest cloud droplets (e.g. Lamer et al., 2020). Smalley and Rapp (2020) addressed this by including CALIPSO measurements, which are sensitive to the smallest cloud droplets, in their identification of contiguous cloudy regions. However for this study, cloud objects must not be missing any reflectivity values. As a result, some cloud object edges may not be the true edge, and some of our defined cloud objects may be connected to other cloud objects.”* has been added on Page 4, Lines 95-100 to address the caveat regarding CloudSat not being sensitive to the smallest non-raining cloud drops.

b. In general, the uncertainty in rain water path varies by pixel depending on path integrated attenuation, uncertainty in cloud water, the drop size distribution, and evaporation. To address this comment, we used the incidence precipitation flag from 2C-PRECIP-COLUMN (Haynes et al. 2009). Specifically, we use the least strict definition of raining pixels (rain possible, probable, and certain) to identify raining pixels within cloud objects, because using the most strict definition of raining pixels (rain certain) biases our results to only larger cloud objects and removes cloud objects that are likely producing light drizzle which are identified using both rain possible and probable. Additionally, Lebsock et al. (2011) used the same three flags to identify raining pixels in their analysis of cloud water to rain water for similar reasons. As a result, we believe using all three rain incidence flags to identify raining pixels and match  $W_p$  to each cloud object. For specifics, see the following text (Page 4, Lines 108-114) which has been added to the paper: *“We use the incidence precipitation flag from 2C-PRECIP-COLUMN (rain possible, probable, or certain) to identify raining cloud objects and the raining pixels within them. Using all three rain flags helps us identify pixels only producing light drizzle that might be evaporating before reaching the surface to those producing heavier rainfall (Haynes et al., 2009). This range of rainfall is incorporated into the integrated precipitation water path product from 2C-RAIN-PROFILE (Lebsock, 2018), and we use this product to determine the average rain water path ( $W_p$ ) for each cloud object, only including  $W_p$  associated with raining pixels in the average.”*

- c. As for cloud water path, we tested the sensitivity of the ratio of cloud water path to rain water path using pixels with no cloud water path threshold, a threshold of  $20 \text{ g m}^{-2}$ , and a threshold of  $30 \text{ g m}^{-2}$  in our calculation of mean cloud object cloud water path. We chose  $20 \text{ g m}^{-2}$  because it was suggested by the reviewer, and  $30 \text{ g m}^{-2}$  as a conservative estimate based on an uncertainty estimate of  $28 \text{ g m}^{-2}$  from Jolivet and Feijt (2005), and an uncertainty estimate of  $36 \text{ g m}^{-2}$  using uncertainties in effective radius and optical thickness from Platnick and Valero (1995). We found that our results do not change based on the cloud water path uncertainty threshold that we use, therefore, based on studies mentioned above, we now only use MODIS pixels with cloud water path  $> 30 \text{ g m}^{-2}$  in our calculation of the ratio of cloud water path to rain water path in this study. See the following text (Page 5, Lines 131-136) that is now in the paper:
- “Given potential uncertainties in  $W_c$ , we tested the sensitivity of our results to only including MODIS pixels with a minimum  $W_c > 0 \text{ g m}^{-2}$ ,  $20 \text{ g m}^{-2}$ , and  $30 \text{ g m}^{-2}$  in our analysis, and we found that the overall interpretation of our results does not change depending on the minimum  $W_c$  threshold used. Even though our overall results do not change using a  $W_c$  threshold below  $30 \text{ g m}^{-2}$ , we use the conservative estimate of  $W_c (\geq 30 \text{ g m}^{-2})$  which is based on an uncertainty estimate of  $28 \text{ g m}^{-2}$  from Jolivet and Feijt (2005), coupled with an estimated uncertainty of  $36 \text{ g m}^{-2}$  which was determined using error in effective radius and optical depth from Platnick and Valero (1995).”*

d. The reason we chose below 3 km relative humidity as our moisture metric is because it was suggested and used in Smalley and Rapp (2020). However, we agree with this reviewer that boundary layer depth will not always be at or above 3 km. For a potentially better representation of boundary layer relative humidity, we tested the sensitivity of our results to relative humidity closer to the surface (850-mb, 925-mb, surface, and average below 850-mb). We found that the interpretation of our results were insensitive to the specific atmospheric level within the boundary layer we use to classify relative humidity. Therefore, we now use average below 850-mb relative humidity, which corresponds to a standard height of 1500 m, as a proxy for boundary-layer relative humidity. For specifics, please see the following text (Page 6, Lines 168-173) which has been added to the paper: *“RH is classified using 6-hourly ECMWF-AUX (Cronk and Partain, 2017). However, because lateral mixing at shallow cumulus edges would most likely be entraining boundary layer air (see review by de Rooy et al., 2013), we tested the sensitivity of our results to RH at different pressure levels (850-mb and 950-mb) in the lower atmosphere, at the surface, and the average RH at or below 850-mb; We found that, while the magnitudes slightly change, the overall interpretation of our results does not depend on our definition of RH. As a result, we classify RH as the average RH at or below 850-mb and match it to each cloud object.”*.

6. The single line in Figure 2 begs for the spread to be shown and statistical significance tests to be performed.<sup>a</sup> The same applies to Figures 3-5.<sup>a</sup> How large is the spread?<sup>a</sup> Are the median lines shown statistically significant?<sup>a</sup> In addition, some numbers and symbols are missing in the legends of Figure 3-5.<sup>b</sup> Lastly, edge lines in Figure 4 are not blue as described in the caption.<sup>c</sup>
  - a. **We now use a monte carlo methodology to estimate the spread in sample median values at a given x value on each figure. We classify error in the median lines as plus/minus one standard deviation surrounding each median value at a given x value on each figure, considering lines significantly different if their associated error bars do not overlap. See the text for details on how we estimate error (Page 7, Lines 204-207): “Note, we estimate the uncertainty in median WRR at any given extent by bootstrapping WRR at a given extent 10,000 times with replacement. Error in WRR median is then classified as  $\pm$  one standard deviation of the bootstrapped sample distribution of median values. Similar error estimates are shown in Figures 3-5 later in this section.”.**
  - b. **See the updated legends in Figures 3-5.**
  - c. **See updated Figure 4 for correction.**
7. Lines 117-119: More important caveats to list than the type of aerosol not being considered are AOD not necessarily scaling with CCN number due to its dependence on size, AOD being offset from the actual clouds, AOD being column integrated such that aerosols may not be making it into the cloud, and AOD being positively correlated with relative humidity due to aerosol swelling.
  - a. **These are definitely important caveats that must be discussed before using AOD to classify the influence of aerosols on warm rain. As a result, we added the following text (Pages 5-6, Lines 159-165) to the paper that accounts for these caveats: “Note that AOD may not necessarily scale with the number of CCN due to its dependence on particle size, and that aerosol type varies globally. Additionally, AOD, being column integrated, does not give any information about where the aerosols are within the atmospheric column, so high AOD does not necessarily mean that aerosols are occurring within the cloud layer. Finally, multiple studies have shown that AOD depends on relative humidity (Su et al., 2008; Michel Flores et al., 2012; Neubauer et al., 2017; Liu and Li, 2018). This results in aerosols swelling due to the uptake of water and an underestimation of the first indirect aerosol effect (Liu and Li, 2018). These conditions are not considered in this study but may factor into WRR.”.**

8. The studies cited on lines 176-177 as supporting the conclusion that more protection from entrainment is what is causing the larger clouds to rain more are not necessarily relevant in that they are analyzing kilometer-scale cumulus congestus and deep convective clouds, not 10 km wide shallow clouds.
  - a. **We removed the reference to Hernandez-Deckers and Sherwood (2018) and replaced it with a reference to Tian and Kuang (2016) which is more applicable to shallow cumulus, and modified the reference to Moser and Lasher-Trapp (2017) for clarity. See the following text (Page 8, lines 236-240) for changes “Narrowing this down to the possible influence of entrainment on cloud object updrafts from cloud edge to center, this is also consistent with previous modeling studies that found larger shallow cumulus cloud cores are more insulated from entrainment (e.g. Burnet and Brenguier, 2010; Tian and Kuang, 2016), a more adiabatic cloud core of developing cumulus as shown in Figure 2 from Moser and Lasher-Trapp (e.g. 2017), and a higher probability of rainfall (e.g. Smalley and Rapp, 2020) in observations.”.**

#### Minor Comments

1. Lines 47-50: Romps (2014) examined precipitation efficiency with respect to relative humidity but relative humidity typically remains approximately constant over oceans as a function of temperature and it is absolute humidity that increases with SST and temperature, so Lau and Wu (2003) is not consistent with Romps (2014) because one is analyzing relative humidity, which impacts evaporation rate, while the other is examining absolute humidity, which impacts condensed mass.
  - a. **Considering we wanted to highlight the potential influences of entrainment on warm rain efficiency, and that would be related to evaporation rates, we have removed the reference to Lau and Wu (2003) as you can see in the updated text (Page 2, Lines 48-51): “Using a model, Romps (2014) found precipitation efficiency to be closely related to RH, defining the lower bound of precipitation efficiency as  $\geq 1 - RH$ . Therefore, the precipitation efficiency at any given level of the atmosphere should increase with increasing RH in response to lower evaporation rates. This suggests that lower RH would result in increased evaporation rates and lower warm rain efficiencies.”.**

2. Lines 50-53: Why are larger droplets necessarily expected near cloud base? Drizzle typically forms first near the top of the cloud in an updraft where the condensed mass and turbulence is greatest. Is it the falling of this drizzle and collection of cloud droplets during falling that produces the largest droplets near cloud base?
  - a. **The expectation is that a more efficient collision-coalescence process at cloud center will result in larger droplets, because the smaller droplets originating at the top of the cloud will fall through cloudy air with a higher amount of cloud water available for drop growth resulting in the largest drops near cloud base (See page 2, Line 42-43 for clarification): “As a result, smaller droplets originating near cloud-top may be more likely to continuously grow larger as they fall, potentially reaching raindrop size near cloud base.”.**
3. Line 58: Please clarify whether cloud water and raindrop concentration refer to number concentration or mass concentration.
  - a. **The reference to Albrecht (1989) refers to cloud water mass concentration, while the reference to Saleeby et al. (2015) refers to raindrop number concentration. We clarified this in the following text (Page 3, Lines 65-69) in the paper: “Albrecht (1989) found that increasing precipitation efficiency within a model is equivalent to decreasing the amount of cloud concentration nuclei (CCN), which reduces the mass concentration of cloud water within a cloudy layer. Similarly, Saleeby et al. (2015) used a cloud model to recently show**
  - b. **that the number concentration of smaller cloud drops increases, but the number concentration of rain drops decrease as CCN increase in the presence of increasing aerosols.”.**
4. Line 66: missing a verb after “aerosol loading”.
  - a. **See the following text (Page 3, Line 76) for this correction: “However, the relationship between cloud water and precipitation as shallow cumulus grow larger, environmental moisture increases, and/or as aerosol loading varies”.**
5. Line 103: Symbol is missing in parentheses.
  - a. **That should have been a reference to (Cronk and Partain, 2018), and see the following text (Page 5, Line 140) for this correction: “As a result,  $W_C$  is then calculated for each CloudSat pixel by averaging the nearest nine non-zero MOD-06-1KM (Platnick et al., 2003) pixels within a 3x3 grid surrounding each CloudSat pixel, which have been previously matched to the CloudSat track in the MOD-06-1KM product (Cronk and Partain, 2018).”.**
6. Line 107: Insert “Rayleigh” before “reflectivity”.

- a. **As is shown in the following text (Page 5, Line 148) now in the paper, we now refer to “reflectivity” as “Rayleigh reflectivity” when it is first discussed in the methods: *“Considering Rayleigh reflectivity is a function of the drop size distribution to the sixth power, it is expected that the maximum reflectivity in non-raining cloud objects will occur near cloud-top, then shift downward as a cloud transitions from non-raining to raining.”***
7. Lines 135-138: More important than relative humidity impacted evaporation to increasing rain water path is absolute humidity, which controls how much condensation occurs.
  - a. **While it is true that absolute humidity is important to the amount of condensation that occurs, We find that relative humidity generally decreases from a median value of approximately 90% in the tropics to a median value of 80% as you move north or south towards the midlatitudes. Considering the large-scale environment (as defined using ECMWF) is generally not saturated, we would argue that relative humidity is the more important metric to reference here because there won’t be any condensation if the environment does not reach saturation. To make this clear, we have modified the following text (Page 6, Lines 186-187) in the paper *“We find that relative humidity generally decreases from median values near 90% in the tropics to median values near 80% north or south into the midlatitudes (not shown), this is consistent with modeling studies that found less cloud water evaporates away in wetter environments (e.g. Tian and Kuang, 2016).”***
8. Lines 146-147: Is “east” supposed to be “west”? And why is “north” used with respect to the ITCZ?
  - a. **It should say that extent decreases to the west from the stratocumulus regions into the trade cumulus regions Additionally, north is being used with respect to the ITCZ to say that the shallow cumulus cloud objects classified by Smalley and Rapp (2020) are also smaller in horizontal size (extent) north of both the trade cumulus and stratocumulus regions within the ITCZ region. To better clarify both of these points, , see the following text (page 7, lines 196-198) that has been modified in the paper: *“Patterns in spatial extent shown in Figure 1d are similar to those found by Smalley and Rapp (2020), who used combined CloudSat/CALIPSO to define extent, with extent decreasing from the stratocumulus regions west into the trade cumulus regions and north of the trade cumulus and stratocumulus regions into the ITCZ.”***

9. Line 160: Be more specific than “environmental moisture”. This implies absolute humidity but in fact what is analyzed is relative humidity.
  - a. **We changed instances of “environmental moisture” in the abstract, results, and conclusions to “RH” (average RH at or below 850-mb).**
10. Lines 165-168: The different vertical gradients of reflectivity near cloud edges as compared to near cloud centers does not conclusively show that larger droplets are present near cloud base at cloud center than on the edge because we don’t know the absolute reflectivity magnitudes.
  - a. **We added a panel to Figure 4 (now Figure 4b) to show how reflectivity values near cloud base change from cloud object center to cloud object edge, and added the following text to pages 7-8, lines 224-229: “Figure 4b confirms that cloud drops are largest near cloud object center, with a median reflectivity of -5.28 dBZ. Reflectivity values, and subsequent drop sizes, then decrease moving from cloud object center to cloud object edge, with edge values of -17.96 dBZ. Figure 4a coupled with 4b implies, at least for extents of 8.4 km, drops grow larger near cloud object centers and may be more protected from mixing.”.**

## References:

- Klein, S. A. and Hartmann, D. L.: The Seasonal Cycle of Low Stratiform Clouds, *Journal of Climate*, 6, 1587–1606, [https://doi.org/10.1175/1520-0442\(1993\)006<1587:TSCOLS>2.0.CO;2](https://doi.org/10.1175/1520-0442(1993)006<1587:TSCOLS>2.0.CO;2), [https://doi.org/10.1175/1520-0442\(1993\)006<1587:TSCOLS>2.0.CO;2](https://doi.org/10.1175/1520-0442(1993)006<1587:TSCOLS>2.0.CO;2), 1993.
- Smalley, K. M. and Rapp, A. D.: The role of cloud size and environmental moisture in shallow cumulus precipitation, *Journal of Applied Meteorology and Climatology*, 0, null, <https://doi.org/10.1175/JAMC-D-19-0145.1>, <https://doi.org/10.1175/JAMC-D-19-0145.1>, 2020
- Haynes, J. M., L’Ecuyer, T. S., Stephens, G. L., Miller, S. D., Mitrescu, C., Wood, N. B., and Tanelli, S.: Rainfall retrieval over the ocean with spaceborne W-band radar, *Journal of Geophysical Research*, 114, <https://doi.org/10.1029/2008jd009973>, <https://doi.org/10.1029/2008jd009973>, 2009.
- Lebsock, M. D., L’Ecuyer, T. S., and Stephens, G. L.: Detecting the Ratio of Rain and Cloud Water in Low-Latitude Shallow Marine 465 Clouds, *Journal of Applied Meteorology and Climatology*, 50, 419–432, <https://doi.org/10.1175/2010JAMC2494.1>, <https://doi.org/10.1175/2010JAMC2494.1>, 2011.
- Jolivet, D. and Feijt, A. J.: Quantification of the accuracy of liquid water path fields derived from NOAA 16 advanced very high resolution radiometer over three ground stations using microwave radiometers, *Journal of Geophysical Research: Atmospheres*, 110,

<https://doi.org/https://doi.org/10.1029/2004JD005205>,  
<https://agupubs.onlinelibrary.wiley.com/doi/abs/10.1029/2004JD005205>, 2005.

Platnick, S. and Valero, F. P. J.: A Validation of a Satellite Cloud Retrieval during ASTEX, *Journal of the Atmospheric Sciences*, 52, 2985–3001,  
[https://doi.org/10.1175/1520-0469\(1995\)052<2985:AVOASC>2.0.CO;2](https://doi.org/10.1175/1520-0469(1995)052<2985:AVOASC>2.0.CO;2), [https://doi.org/10.1175/1520-0469\(1995\)052<2985:AVOASC>2.0.CO;2](https://doi.org/10.1175/1520-0469(1995)052<2985:AVOASC>2.0.CO;2), 1995.

Tian, Y. and Kuang, Z.: Dependence of entrainment in shallow cumulus convection on vertical velocity and distance to cloud edge, *Geophysical Research Letters*, 43, 4056–4065,  
<https://doi.org/10.1002/2016gl069005>, <https://doi.org/10.1002%2F2016gl069005>, 2016.

Hernandez-Deckers, D. and Sherwood, S. C.: On the Role of Entrainment in the Fate of Cumulus Thermals, *Journal of the Atmospheric Sciences*, 75, 3911–3924, <https://doi.org/10.1175/jas-d-18-0077.1>,  
<https://doi.org/10.1175%2Fjas-d-18-0077.1>, 2018.

Moser, D. H. and Lasher-Trapp, S.: The Influence of Successive Thermals on Entrainment and Dilution in a Simulated Cumulus Congestus, *Journal of the Atmospheric Sciences*, 74, 375–392,  
<https://doi.org/10.1175/JAS-D-16-0144.1>, <https://doi.org/10.1175/JAS-D-16-0144.1>, 2017.

Lau, K. M. and Wu, H. T.: Warm rain processes over tropical oceans and climate implications, *Geophysical Research Letters*, 30, <https://doi.org/10.1029/2003GL018567>,  
<https://agupubs.onlinelibrary.wiley.com/doi/abs/10.1029/2003GL018567>, 2003.

Albrecht, B. A.: Aerosols, Cloud Microphysics, and Fractional Cloudiness, *Science*, 245, 1227–1230,  
<https://doi.org/10.1126/science.245.4923.1227>,  
<https://science.sciencemag.org/content/245/4923/1227>, 1989.

Saleeby, S. M., Herbener, S. R., van den Heever, S. C., and L'Ecuyer, T.: Impacts of Cloud Droplet–Nucleating Aerosols on Shallow Tropical Convection, *Journal of the Atmospheric Sciences*, 72, 1369–1385, <https://doi.org/10.1175/JAS-D-14-0153.1>, <https://doi.org/10.1175/JAS-D-14-0153.1>, 2015.

Cronk, H. and Partain, P.: CloudSat ECMWF-AUX Auxillary Data Product Process Description and Interface Control Document, Tech. rep., Colorado State University, 2017.

## Reviewer 2

We appreciate the reviewer's helpful comments and suggestions that helped us improve this manuscript. Reviewer comments are in black. Our responses are red, and the updated text shown in this document is blue.

This paper is a useful analysis of the production of warm rain in cumulus clouds based primarily on cloud and rain water measurements from the CloudSat and MODIS satellite datasets. The main new result is that the efficiency of production of warm rain appears to increase with the horizontal size of the cloud, even when controlling for variations in cloud depth and sea surface temperature. The results imply that dilution of cloud updrafts due to entrainment is less effective in larger clouds than smaller clouds which are presumably better protected by the larger scale of the clouds. This is a plausible hypothesis supported by some prior modeling. The paper shows consistent results between an examination of the ratio of precipitation water to cloud water and the vertical gradient in CloudSat reflectivity. I have some comments about the resolution of the measurements used, the quantification of "warm rain efficiency", and the conclusions the authors draw about the aerosol sensitivity of warm rain efficiency. The paper should be suitable for publication in ACP subject to some revisions.

## Major Comments

1. Some aspects of the scales of the clouds in this investigation are left unanswered, but are potentially critical because of the resolution of the measurements employed. The CloudSat rain water data used here has a footprint of 1.4 x 1.8 km. The cloudwater path data from MODIS has a nominal resolution of ~1 km at nadir. According To the methods, the cloud water path is based on a 9-pixel average, which suggests that the horizontal scale of the cloud water measurements are on the scale of 10 km. Nevertheless, clouds are shown varying from about 1.7 km to greater than 18 km. So,one question is: are the cloud water values really representative of the true values for clouds smaller than 10 km? Can we then be certain that the strong dependence of the ratio of precipitation water to cloud water on cloud scale shown in figure 2 for clouds smaller than 10 km is not influenced by the resolution of the cloud water quantity?

- a. **To address the reviewer's concerns, we used a 3x3 grid (nine pixel) average surrounding each CloudSat pixel and only averaged cloud water path values that are  $> 0 \text{ g m}^{-2}$ . We did this, because one CloudSat Pixel could overlap multiple MODIS pixels within that 3x3 grid, meaning that an average of multiple pixels is the best way to match MODIS cloud water path to each CloudSat pixel. However, we tested our results to check if matching the nearest pixel or nearest nine pixels would impact our results. We found that our results are consistent no matter what method is used to match MODIS cloud water path. To address this, the following text has been modified in the methods to clarify how we match cloud water path to each CloudSat pixel and mention that matching both a nine-pixel average and nearest-neighbor cloud water path does not change our overall results (Page 5, Lines 136-143) *"Due to horizontal resolution differences between CloudSat and MODIS, one CloudSat pixel may overlap multiple MODIS pixels within a surrounding 3x3 km grid. As a result,  $W_c$  is then calculated for each CloudSat pixel by averaging the nearest nine non-zero MOD-06-1KM (Platnick et al. 2003) pixels within a 3x3 grid surrounding each CloudSat pixel, which have been previously matched to the CloudSat track in the MOD-06-1KM product (Cronk and Platnick, 2018). There could be concerns that the averaging  $W_c$  within the nearest nine MODIS pixels may not properly represent the  $W_c$  at the appropriate scales relative to the horizontal footprint of each CloudSat pixel, however we tested our results using  $W_c$  within the nearest MODIS pixel and found that our overall results do not change."***
2. The authors state that "prior studies [of biases in MODIS cloud water] have found them to be small in comparison to other satellite retrievals". I suspect that this result may be resolution dependent and that in fact uncertainties for cloud smaller than several km in scale may be quite significant. For example, Cho et al. (2015) find that the MODIS cloud property retrievals from which the cloud water path is derived can have substantial errors in cumulus cloud fields because of partially cloudy pixels and horizontal homogeneity of cloud properties within the satellite footprint. Can the authors provide some greater support for the notion that the cloud water values are representative of the true value at the scales on the small end of the spectrum shown in this analysis?

- a. Thank-you for pointing out Cho et al. (2015) and that failure rates are higher in regions of broken cumulus. This should have been highlighted and caveated in the manuscript. Therefore we modified the following text (Pages 4-5, Lines 121-131) to account for this: *“Cho et al. (2015) found that MODIS effective radius and optical depth retrieval failure rates are higher in regions of broken trade cumulus than regions of predominantly stratocumulus, and they primarily attributed this to the presence of partially filled and inhomogeneous cloudy pixels. They also found that a large fraction of unexplained MODIS retrieval failures are related to the presence of precipitation after comparing MODIS failure rates to non-precipitating and precipitating pixels classified by CloudSat. This is attributed to a higher frequency of failures due to effective radius being too large. Considering the retrieval of effective radius and optical depth are required to derive  $W_c$  and higher failure rates within broken trade cumulus, we suspect unavoidable sampling bias exists in  $W_c$  matched to the smallest cloud objects and/or those containing large droplets and heavy rain. However on a global scale, prior studies have found the uncertainties in MODIS  $W_c$  are small in comparison to other satellite retrievals (Seethala and Horvath, 2010; Lebsock and Su, 2014), with the global mean of MODIS  $W_c$  being within  $5 \text{ g m}^{-2}$  of  $W_c$  determined using the Advanced Microwave Scanning Radiometer for Earth Observing System (AMSR-E) (Seethala and Horvath, 2010).”*
3. Fine resolution satellite imagery indicates that warm cumulus clouds substantially smaller than 1.7 km are common and in fact may be more prevalent than clouds larger than 1.7 km (e.g. Mieslinger et al. 2019). Presumably some of these clouds may be precipitated. Obviously, comparable data to the CloudSat data are not available at smaller scales from satellites. Nevertheless, do the authors expect that there may be a substantial population of precipitating cumulus clouds that are not captured in their analysis? Furthermore, one might expect that warm cumulus clouds might be limited inscale. Assuming crudely that cumulus clouds typically have an aspect ratio of around 1, one might presume that cumulus clouds broader than 5-10 km might also be tall enough to contain ice or mixed phase microphysical processes occurring. What characteristics ensure that the clouds included here are both warm liquid phase and truly cumulus clouds, or is the analysis expecting to include some stratocumulus clouds as well?

- a. **The reviewer is correct in assuming that there is likely a large population of raining shallow cumulus smaller than CloudSat can detect leading to non-uniform beam filling. To address this (Pages 9-10, Lines 288-294) see the following text: “At the small end of the shallow cumulus horizontal size spectrum, CloudSat is limited to observing cloud objects no smaller than 1.4 x 1.8 km. Given prior ground observational studies, it is likely that there is a significant population of shallow cumulus cloud objects not identified by our study (e.g. Kollias et al., 2003; Mieslinger et al., 2019) due to non-uniform beam filling effects. Battaglia et al. (2020) noted that this results in an underestimation of path integrated attenuation, potentially introducing error into the retrieval of  $W_p$ . Unfortunately, this limitation is unavoidable given CloudSat’s horizontal resolution.”.**
- b. **To address the potential issue of mixed phase clouds, we now explain in the following text (Page 4, lines 104-107) how we ensure that our analysis only includes warm cloud objects “To ensure that none of the cloud objects examined here contain ice, we only include cloud objects with tops entirely below the freezing level as defined in 2C-PRECIP-COLUMN Haynes et al. 2009).”**

4. The authors use the ratio of precipitation water to cloud water as their measure of “warm rain efficiency”. Although, as the authors note, this quantity is just a proxy for the true efficiency. I think the authors are correct to make this point clear. I also think that perhaps it would be helpful for the authors to clarify what defines a proper quantitative measure of the warm rain efficiency. Presumably, it is not so easily observed, which is why they have chosen a proxy, which is fine. Given the brevity of this paper, however, I think a short elaboration on this point would be helpful. Furthermore, if the ratio used in this paper is merely a proxy for the true efficiency, is it really appropriate to be using “warm rain efficiency” throughout the manuscript to refer to this quantity? I suggest that the authors perhaps consider a different name so that readers are not confused about what is the true measure of the efficiency and what is the approximation of it. Alternatively, if there is a quantitative comparison of the ratio to the true efficiency, perhaps from a theoretical study, then it might be appropriate to refer to the proxy value as a measure of the efficiency with some quoted uncertainty value.

a. **We agree that we should have defined warm rain efficiency in a proper context, therefore we added the following text (Pages 2-3, Lines 51-59) to the paper:** *“Prior studies have defined precipitation efficiency in two ways: 1) as the large-scale precipitation efficiency and 2) as the cloud microphysical precipitation efficiency. Generally, observational studies have based their definition of precipitation efficiency on the large-scale definition, which has simply been defined as the ratio of surface rain rate to the sum of both vapor mass flux in/out of a cloud and surface evaporation (e.g. Chong and Hauser, 1989; Tao et al., 2004; Sui et al., 2007), whereas the cloud microphysical definition, or the ratio of surface rain rate to the sum of vapor condensation and deposition rates, has been primarily used in cloud modeling studies (e.g. Li et al., 2002; Sui et al., 2005; Gao et al., 2018). Although both the large-scale and cloud microphysical definitions of precipitation efficiency are useful (Sui et al., 2005; Sui et al., 2007), variations in the ratio of cloud water to rain water (WRR) in response to changes in evaporation can theoretically be used as a proxy for warm rain efficiency based on the cloud microphysical definition.”* **Additionally, we changed any reference to WRE, in the context of this paper, to the ratio of cloud water to rain water (WRR) as well as “warm rain efficiency” in the title to “the ratio of cloud water to rain water”.**

5. The corroboration of the inferences based on the ratio of precipitating water to cloudwater with the inferences from the vertical gradient in reflectivity (VGZ) is a valuable contribution of this paper and certainly strengthens the case that the authors are making. In lines 174 to 180 the authors argue that the dependence of VGZ on cloud-top height supports the notion that updrafts in larger clouds are protected from entrainment. Why would this dependence on cloud-top height not simply result from collision/coalescence happening through a deeper cloud layer independent of any difference in entrainment? Presumably the taller clouds are provide a broader distance from cloud base to cloud top through which raining drops can fall and collect cloud drops. Likewise, perhaps a stronger updraft that yields a taller cloud is better at promoting the coalescence of cloud drops through turbulent collisions. Could these similarly explain the differences between clouds of differing heights?

- a. Yes, these factors could also explain differences in VGZ as a function of extent as well as differences in the ratio of cloud water to rain water for cloud objects with different heights. To address this we added the following text in a section called “*Limitations of analysis and observations*” to our paper (Page 9, Lines 268-287)
- “This study has emphasized the potential for the decreasing impact of entrainment on cloud cores, resulting in higher WRR, as cloud size increases; however, it is important to point out other factors related to cloud size that may also impact WRR. Figure 3 shows WRR is higher when cloud objects are taller, which may be simply because we are sampling more mature clouds that have had more time for the collision-coalescence process to result in rain formation. Deeper shallow cumulus not only live longer which would give cloud droplets more time to grow to raindrop size (e.g. Burnet and Brenguier, 2010), but they are more likely to have more intense updrafts which could result in more water vapor being transported to higher altitudes within a cloud. Stronger updrafts are then more likely to be able to suspend cloud droplets higher in the cloud for longer periods of time which allows them to grow larger before they begin to fall and collision-coalescence is initiated. Once cloud droplets do begin to fall, they are not only potentially larger but able to collect more droplets over a larger distance than droplets falling through a shallower cloud. This could potentially result in higher WRR, however there is likely a lag between the peaks in cloud water path and rain water path as cloud drops grow to raindrop size in a developing cloud. Earlier modeling studies have also noted that turbulent flow potentially enhances the likelihood of warm rain formation (e.g. Brenguier and Chaumat, 2001; Seifert et al., 2010; Wyszogrodzki et al., 2013; Franklin, 2014; Seifert and Onishi, 2016; Chen et al., 2018). Seifert et al. (2010) found that turbulence effects are largest near cloud tops in shallow cumulus, which they note is an important region for initial rain formation. While these additional processes may impact WRR, the satellite observations used in this study are instantaneous snapshots in time. We attempted to remove some of these life cycle impacts by binning cloud objects by top height. Within a given cloud top height bin, WRR (Figure 3) and the magnitude of  $VGZ_{CP}$  (Figure 4c) still increase as a function of extent. While we acknowledge that this cannot fully remove these impacts, these results support the idea that processes other than those related to cloud lifetime, like lateral entrainment, may also influence*

***the WRR of shallow cumulus of different horizontal sizes”.***

6. Finally, the authors explore the dependence of their proxy for warm rain efficiency on the aerosol optical thickness in the vicinity of the cloud. They conclude that there is little dependence of the efficiency on aerosols, which is an interesting result. I suggest, though, that the authors remove the word “surprisingly” from the abstract where this result is reported. As noted by the authors, by excluding non-precipitating clouds from their analysis they are likely missing the expected dominant effect, which is the suppression of rain formation. Is there not a CloudSat study looking at the dependence of the occurrence of rain in CloudSat retrievals upon AOD? I think that a citation to such a study would be appropriate in the discussion of the results presented in this paper. If not, I think the authors should point out that this might be the more fruitful path to quantifying aerosol effects.

- a. **We have removed “surprisingly” from the abstract**
- b. **To address the second part of your comment regarding the dependence of the occurrence of rain in CloudSat retrievals upon AOD, we added a figure (Figure 5d) which shows the rain likelihood determined using CloudSat cloud objects at a given AOD. For reference, it is described in the following text on Pages 8-9, Lines 261-264: “Figure 5d shows the likelihood of rain occurrence at a given AOD determined by the ratio of raining cloud objects to the total number of cloud objects. As expected, Figure 5d shows that the likelihood of rain decreases as AOD increases, with rain likelihood of about 50% in the cleanest environments decreasing to about 40% for an AOD approaching 0.75. These results imply that once the condensation-coalescence is initiated, aerosol loading has a smaller impact on the conversion of cloud water to rain than other cloud or environmental characteristics.”.**

## References:

- Cho, H.-M., Zhang, Z., Meyer, K., Lebsock, M., Platnick, S., Ackerman, A. S., Di Girolamo, L., C.-Labonnote, L., Cornet, C., Riedi, J., and Holz, R. E.: Frequency and causes of failed MODIS cloud property retrievals for liquid phase clouds over global oceans, *Journal of Geophysical Research: Atmospheres*, 120, 4132–4154, <https://doi.org/https://doi.org/10.1002/2015JD023161>, <https://agupubs.onlinelibrary.wiley.com/doi/abs/10.1002/2015JD023161>, 2015.

# A-Train estimates of the sensitivity of ~~warm~~ the cloud to rain likelihood and efficiency water ratio to cloud size, ~~environmental moisture~~ relative humidity, and aerosols

Kevin M. Smalley<sup>1</sup> and Anita D. Rapp<sup>1</sup>

<sup>1</sup>Department of Atmospheric Sciences, Texas A&M University, College Station, Texas

**Correspondence:** Kevin M. Smalley (ksmalley@jpl.nasa.gov)

**Abstract.** Precipitation efficiency has been found to play an important role in constraining the sensitivity of the climate through its role in controlling cloud cover, yet understanding of its controls are not fully understood. Here we use CloudSat observations to identify individual contiguous shallow cumulus cloud objects and compute the ratio of cloud water path to rain water (WRR) path as a proxy for warm rain efficiency (~~WRE~~). Cloud objects are then conditionally sampled by cloud-top height, relative humidity, and aerosol optical depth (AOD) to analyze changes in ~~WRE~~ WRR as a function of cloud size (extent). For a fixed cloud-top height, ~~WRE~~ WRR increases with extent and environmental humidity following a double power-law distribution, as a function of extent. Similarly, ~~WRE increases holding environmental moisture~~ WRR increases holding average relative humidity at or below 850-mb constant. There is ~~surprisingly~~ little relationship between ~~WRE~~ WRR and AOD when conditioned by cloud-top height, suggesting that once rain drop formation begins, aerosols may not be as important for ~~WRE~~ WRR as cloud size and depth. Consistent with prior studies, results show an increase in ~~WRE~~ WRR with sea surface temperature. However, for a given depth and SST, ~~WRE~~ WRR is also dependent on cloud size and becomes larger as cloud size increases. Given that larger objects become more frequent with increasing SST, these results imply that increasing precipitation efficiencies with SST are due not only to deeper clouds with greater cloud water contents, but also the propensity for larger clouds which may have more protected updrafts.

15 *Copyright statement.* TEXT

## 1 Introduction

Low cloud cover continues to be a dominant source of uncertainty in projecting future climate (e.g. Bony and Dufresne, 2005; Dufresne and Bony, 2008; Vial et al., 2013), with variations in shallow cumulus distributions explaining much of the differences in climate model-derived estimates of climate sensitivity (e.g. Wyant et al., 2006; Medeiros and Stevens, 2011; 20 Nam et al., 2012). This stems from climate models' inability to simulate shallow cumulus and their impacts, due in part to the low temporal and spatial resolution of these models (e.g. Stevens et al., 2002), as well as the fact that small-scale processes important for cloud development, including turbulence and convection, must be parameterized (e.g. Tiedtke, 1989; Zhang and

McFarlane, 1995; Bretherton et al., 2004). Studies have shown precipitation efficiency is a key parameter used to constrain cloud parameterizations within climate models (Rennó et al., 1994; Del Genio et al., 2005; Zhao, 2014; Lutsko and Cronin, 2018). Nam et al. (2012) hypothesized that shallow cumulus are too reflective in climate models, possibly because model precipitation efficiencies are too weak. This results in excess cloud water which increases cloud optical depth and shallow cumulus reflectance. Prior observational and modeling studies found the precipitation efficiency of shallow cumulus increases as sea-surface temperature (SST) increases in response to climate change (Lau and Wu, 2003; Bailey et al., 2015; Lutsko and Cronin, 2018). Factors including environmental moisture (e.g. Heus and Jonker, 2008; Schmeissner et al., 2015), entrainment (e.g. Korolev et al., 2016; Pinsky et al., 2016b, a), and aerosols (e.g. Koren et al., 2014; Dagan et al., 2016; Jung et al., 2016b, a) help regulate both thermodynamic and dynamical processes that promote favorable conditions important to not only warm rain production, but also the efficiency of the conversion of cloud water to precipitation. To better constrain cloud parameterizations of these processes and subsequently climate sensitivity to low cloud cover, more observations-based studies analyzing physical processes influencing warm rain efficiencies are needed.

In an ideal shallow cumulus cloud, liquid water content increases adiabatically from cloud base to top. However, liquid water content is generally only 50% - 80% of the adiabatic values due to entrainment (Gerber et al., 2008)(Gerber et al., 2008; Blyth et al., 2013; Y. . Evaporation induced by cloud-edge mixing not only impacts shallow cumulus updraft strength, but also the number and size of droplets within a cloud (Lu et al., 2012), with increased evaporation potentially reducing the number and size of available droplets. Using a large-eddy simulation (LES), Moser and Lasher-Trapp (2017) found the influence of entrainment decreases from cloud-edge to center of individual shallow cumulus as they grow larger. This results in liquid water content at cloud center being closer to adiabatic in larger clouds, because fewer droplets evaporate away at cloud-center. This implies that the collision-coalescence process is more efficient at cloud center, because there is more cloud water available to be collected by large droplets. As a result, smaller droplets originating near cloud-top may be more likely to continuously grow larger as they fall, potentially reaching raindrop size near cloud base. At cloud edge, there are not only fewer droplets but also smaller droplets, potentially reducing collision-coalescence efficiencies there. This is consistent with other LES results that found shallow cumulus updrafts are more insulated from entrainment as they increase in size (e.g. Heus and Jonker, 2008; Burnet and Brenguier, 2010; Tian and Kuang, 2016). LES and limited field-campaign observational studies have shown that cloud updrafts not only become more protected as cloud size increases, but also as ~~environmental moisture increases (Heus and Jonker, 2008; Schmeissner et al., 2015; Hernandez-Deckers and Sherwood, 2018). Romps (2014) used a cloud model to show that precipitation efficiency decreases as relative humidity decreases, because precipitation evaporates more readily in a drier environment. Considering environmental moisture scales with temperature, this is consistent with results found by Lau and Wu (2003) which show the efficiency of warm rain production increases as SSTs increase using Tropical Rainfall Measuring Mission (TRMM) satellite observations. Given relative humidity (RH) increases (e.g. Heus and Jonker, 2008; Schmeissner et al., 2015),~~ Using a model, Romps (2014) found precipitation efficiency to be closely related to RH, defining the lower bound of precipitation efficiency as  $> 1 - RH$ . Therefore, the precipitation efficiency at any given level of the atmosphere should increase with increasing RH in response to lower evaporation rates. This suggests that lower RH would result in increased evaporation rates and lower warm rain efficiencies. Prior studies have defined precipitation efficiency in two ways: 1) as the large-scale

precipitation efficiency and 2) as the cloud microphysical precipitation efficiency. Generally, observational studies have based their definition of precipitation efficiency on the large-scale definition, which has simply been defined as the ratio of surface rain rate to the sum of both vapor mass flux in/out of a cloud and surface evaporation (e.g. Chong and Hauser, 1989; Tao et al., 2004; Sui et al., 2007), whereas the cloud microphysical definition, or the ratio of surface rain rate to the sum of vapor condensation and deposition rates, has been primarily used in cloud modeling studies (e.g. Sui et al., 2007). Although both the large-scale and cloud microphysical definitions of precipitation efficiency are useful (Sui et al., 2007), variations in the ratio of cloud water to rain water (WRR) in response to changes in evaporation can theoretically be used as a proxy for warm rain efficiency based on the cloud microphysical definition. From this coupled with LES results showing that shallow cumulus updrafts are more protected as clouds grow in size and/or environmental moisture increases, RH increases, we hypothesize larger droplets will be evident closer to the cloud base and increase WRE-WRR in larger cloud objects, because the cloud-core of larger cloud objects is more protected from entrainment.

While perhaps not as important as organization (Minor et al., 2011) or cloud size (Jiang and Feingold, 2006), it is widely understood that aerosol concentrations act to suppress warm rain production (Twomey, 1974; Albrecht, 1989) by increasing the cloud droplet concentration and reducing cloud droplet sizes (Squires, 1958). Albrecht (1989) found that increasing precipitation efficiency within a model is equivalent to decreasing the amount of cloud concentration nuclei (CCN), which reduces the amount mass concentration of cloud water within a cloudy layer. Similarly, Saleeby et al. (2015) used a cloud model to recently find both cloud water and rain drop concentration decreases as cloud concentration nuclei increases show that the number concentration of smaller cloud drops increases, but the number concentration of rain drops decrease as CCN increase in the presence of increasing aerosols. Lebock et al. (2011) used CloudSat and Moderate Resolution Imaging Spectroradiometer (MODIS) observations to show that as drop size decreases, the ratio of rain water to cloud water also decreases. Together, these studies suggest the number of large droplets able to fall at sufficient terminal velocities to initiate collision-coalescence and continue growing to large enough sizes to fall out as rain decreases with increasing aerosol concentrations, which would reduce warm rain efficiency (WRE) WRR.

Observationally, prior Earlier studies have used satellite observations to infer the relationship between precipitation efficiency and both sea-surface temperature (Lau and Wu, 2003) and drop size (Lebock et al., 2011). However, the relationship between cloud water and precipitation as shallow cumulus grow larger, environmental moisture increases, and/or aerosol loading as aerosol loading varies has only been investigated using cloud models (e.g. Moser and Lasher-Trapp, 2017) (e.g. Abel and Shipway, 2007; vanZanten et al., 2011; Franklin, 2014; Saleeby et al., 2015; Moser and Lasher-Trapp, 2017; Hoffmann et al., 2010) and limited field-campaign observations (e.g. Gerber et al., 2008) (e.g. Rauber et al., 2007; Gerber et al., 2008; Burnet and Brenguier, 2010). While these case and model studies provide insight into the physical processes, it is unclear how well they represent the shallow cumulus clouds observed globally. Satellites can observe a large enough sample size of shallow cumulus over different regions and during different stages of their lifecycle to gain a more holistic view of this relationship. Prior studies have used TRMM and Global Precipitation Measurement Mission (GPM) observations to analyze warm rain production and efficiency (e.g. Lau and Wu, 2003). Unfortunately, TRMM and GPM are precipitation radars operating at the Ku- and Ka-bands not capable of observing the non-raining portions of clouds or light precipitation. Building off work in Smalley and Rapp (2020)

that analyzed the relationship between rain likelihood and cloud size, this study uses the higher sensitivity radar of CloudSat in addition to MODIS observations to test the hypothesis that *WRE-WRR is higher in larger shallow cumulus and is modulated by environmental moisture RH and aerosol loading.*

## 2 Data and Methods

To determine if larger shallow cumulus clouds are more efficient at producing warm rainfall, this study uses the CloudSat Cloud Profiling Radar (CPR; Tanelli et al., 2008) to identify individual contiguous shallow cumulus cloud objects. The CPR is a near-nadir pointing 94-GHz radar that can observe raining and non-raining cloud drops. It allows us to analyze the horizontal distribution of cloud within a horizontal footprint of 1.4 x 1.8 km, and the vertical distributions of clouds within a 240 m bin within each cloudsat pixel.

Contiguous cloudy regions are initially identified using the 2B-GEOPROF (Marchand et al., 2008) cloud mask confidence values  $\geq 20$ , which removes orbit elements that may be influenced by ground clutter (Marchand et al., 2008). An additional limitation of CloudSat is it's inability to sense the smallest cloud droplets (e.g. Lamer et al., 2020). Smalley and Rapp (2020) addressed this by including CALIPSO measurements, which are sensitive to the smallest cloud droplets, in their identification of contiguous cloudy regions. However for this study, cloud objects must not be missing any reflectivity values. As a result, some cloud object edges may not be the true edge, and some of our defined cloud objects may be connected to other cloud objects. Before identifying cloud objects, 2C-RAIN-PROFILE (Lebsock and L'Ecuyer, 2011) modeled reflectivity is mapped onto the two-dimensional cloud mask field. As outlined by prior literature (e.g. L'Ecuyer and Stephens, 2002; Mitrescu et al., 2010; Lebsock and L'Ecuyer, 2011), modeled reflectivity adjusts the raw reflectivity for multi-scattering and attenuation when it is raining. As described by Smalley and Rapp (2020), we use a lower-tropospheric stability threshold of 18.55 K (?) to separate cloud objects occurring in environments favoring stratocumulus development from those occurring in environments favoring shallow cumulus development. To ensure that none of the cloud objects examined here contain ice, we only include cloud objects with tops entirely below the freezing level as defined in 2C-PRECIP-COLUMN (Haynes et al., 2009). Shallow cumulus cloud objects are then identified using the methodology described by Smalley and Rapp (2020) using the combined two-dimensional reflectivity field, with only single-layer cloud objects included. ~~This study uses 2C-RAIN-PROFILE~~ We use the incidence precipitation flag from 2C-PRECIP-COLUMN (rain possible, probable, or certain) to identify raining cloud objects and the raining pixels within them. Using all three rain flags helps us identify pixels only producing light drizzle that might be evaporating before reaching the surface to those producing heavier rainfall (Haynes et al., 2009). This range of rainfall is incorporated into the integrated precipitation water path product from 2C-RAIN-PROFILE (Lebsock, 2018), and we use this product to determine the average rain water path ( $W_P$ )  $> 0$  to identify raining cloud objects and does not consider non-raining objects  $P$ ) for each cloud object, only including  $W_P$  associated with raining pixels in the average. We then store the median cloud-top height and maximum along-track extent (hereby extent) of each cloud object for later analysis.

Although CloudSat 2B-CWC-RVOD (Austin et al., 2009) does provide a cloud water path ( $W_C$ ) product, the rain drop size distribution used in 2B-CWC-RVOD is not the same as that used in 2C-RAIN-PROFILE. Additionally, Christensen et al.

(2013) found that the 2B-CWC-RVOD algorithm struggles to filter out precipitation sized droplets in the presence of light precipitation and drizzle, which results in an overestimation of cloud water. This, coupled with differences in assumed drop size distributions by 2B-CWC-RVOD and 2C-RAIN-PROFILE, makes 2B-CWC-RVOD  $W_C$  not ideal for this study, so we instead use MODIS  $W_C$ . ~~While there are biases in MODIS shallow cumulus~~ Cho et al. (2015) found that MODIS effective radius and optical depth retrieval failure rates are higher in regions of broken trade cumulus than regions of predominantly stratocumulus, and they primarily attributed this to the presence of partially filled and inhomogeneous cloudy pixels. They also found that a large fraction of unexplained MODIS retrieval failures are related to the presence of precipitation after comparing MODIS failure rates to non-precipitating and precipitating pixels classified by CloudSat. This is attributed to a higher frequency of failures due to effective radius being too large. Considering the retrieval of effective radius and optical depth are required to derive  $W_C$  and higher failure rates within broken trade cumulus, we suspect unavoidable sampling bias exists in  $W_C$  matched to the smallest cloud objects and/or those containing large droplets and heavy rain. However on a global scale, prior studies have found ~~them to be the~~ uncertainties in MODIS  $W_C$  are small in comparison to other satellite retrievals (e.g. Lebrock and Su, 2014). (e.g. Seethala and Horvath, 2010; Lebrock and Su, 2014), with the global mean of MODIS  $W_C$  being within  $5 \text{ g m}^{-2}$  of  $W_C$  determined using the Advanced Microwave Scanning Radiometer for Earth Observing System (AMSRE) (Seethala and Horvath, 2010). Given potential uncertainties in  $W_C$ , we tested the sensitivity of our results to only including MODIS pixels with a minimum  $W_C > 0 \text{ g m}^{-2}$ ,  $20 \text{ g m}^{-2}$ , and  $30 \text{ g m}^{-2}$  in our analysis, and we found that the overall interpretation of our results does not change depending on the minimum  $W_C$  threshold used. Even though our overall results do not change using a  $W_C$  threshold below  $30 \text{ g m}^{-2}$ , we use the conservative estimate of  $W_C (> 30 \text{ g m}^{-2})$  which is based on an uncertainty estimate of  $28 \text{ g m}^{-2}$  from Jolivet and Feijt (2005), coupled with an estimated uncertainty of  $36 \text{ g m}^{-2}$  which was determined using error in effective radius and optical depth from Platnick and Valero (1995). Due to horizontal resolution differences between CloudSat and MODIS, one CloudSat pixel may overlap multiple MODIS pixels within a surrounding  $3 \times 3 \text{ km}$  grid. As a result,  $W_C$  is then calculated for each CloudSat pixel by averaging the nearest nine non-zero MODIS-06-1KM (Platnick et al., 2003) pixels within a  $3 \times 3$  grid surrounding each CloudSat pixel, which have been previously matched to the CloudSat track in the MODIS-06-1KM product (?). (Cronk and Partain, 2018). There could be concerns that the averaging  $W_C$  within the nearest nine MODIS pixels may not properly represent the  $W_C$  at the appropriate scales relative to the horizontal footprint of each CloudSat pixel, however we tested our results using  $W_C$  within the nearest MODIS pixel and found that our overall results do not change. We then store and analyze the median-mean  $W_C$  associated with each cloud object.

~~WRE-WRR~~ of each shallow cumulus cloud object is calculated as  $\frac{W_p}{W_C}$ . Note, this is a proxy for true ~~WRE~~ warm rain efficiency, because mass flux of water in and out of a cloud cannot be determined without a model, ~~however;~~ however, this ratio has been used by prior observational studies to analyze the amount of cloud water converted to rain water (e.g. Lebrock et al., 2011).

Considering Rayleigh reflectivity is a function of the drop size distribution to the sixth power, it is expected that the maximum reflectivity in non-raining cloud objects will occur near cloud-top, then shift downward as a cloud transitions from non-raining to raining. Wang et al. (2017) used the vertical reflectivity gradient (VGZ) to investigate warm rain onset. They found VGZ (positive down) reverses sign (positive to negative) when clouds transition from non-raining to raining. Given previous studies

and results shown in Smalley and Rapp (2020) finding rain is more likely as clouds grow larger in extent, it is hypothesized that the negative VGZ within individual raining cloud objects will increase in magnitude as cloud objects increase in extent. The methodology developed by Wang et al. (2017) is applied to find the VGZ for each pixel within every shallow cumulus cloud object. VGZ at cloud object center pixel ( $VGZ_{CP}$ ) will then be compared to VGZ at cloud object edge pixel ( $VGZ_{EP}$ ) to infer the impact of mixing on cloud object cores as a function of cloud size and ~~environmental moisture~~RH.

The influence of aerosols on the relationship between ~~WRE~~WRR and cloud object ~~efficiency~~size are determined using Aqua MODIS level-3 daily 550 nm aerosol optical depth (AOD) (Ruiz-Arias et al., 2013). Each cloud object is matched to the nearest  $1^\circ \times 1^\circ$  gridbox AOD value. Note ~~, this study does not consider the type of aerosol present in each environment, however this may also factor into the WRE~~that AOD may not necessarily scale with the number of CCN due to its dependence on particle size, and ~~that aerosol type varies globally. Additionally, AOD, being column integrated, does not give any information about where the aerosols are within the atmospheric column, so high AOD does not necessarily mean that aerosols are occurring within the cloud layer. Finally, multiple studies have shown that AOD depends on relative humidity (Su et al., 2008; Michel Flores et al., 2012; Neubauer et al., 2018). This results in aerosols swelling due to the uptake of water and an underestimation of the first indirect aerosol effect (Liu and Li, 2018). These conditions are not considered in this study but may factor into WRR.~~

~~Similar to Smalley and Rapp (2020),~~ As in Smalley and Rapp (2020), this analysis is constrained to only marine shallow cumulus between between 60 N and 60 S. Measurements are constricted to June 2006 and December 2010 because Cloud-Sat stopped taking night time measurements after 2010 due to a battery anomaly (Witkowski et al., 2012). ~~Environmental moisture~~RH is classified using 6-hourly ECMWF-AUX (Cronk and Partain, 2017)~~average relative humidity below 3 km matched~~. ~~However, because lateral mixing at shallow cumulus edges would most likely be entraining boundary layer air (see review by de Rooy et al., 2013), we tested the sensitivity of our results to RH at different pressure levels (850-mb and 950-mb) in the lower atmosphere, at the surface, and the average RH at or below 850-mb. We found that, while the magnitudes slightly change, the overall interpretation of our results does not depend on our definition of RH. As a result, we classify RH as the average RH at or below 850-mb and match it~~ to each cloud object. Cloud-top height, ~~environmental moisture~~RH, VGZ, and AOD are used to control and analyze the relationship between ~~WRE~~WRR and cloud object extent.

### 185 3 Warm rain relationship to extent

Similar to Smalley and Rapp (2020), The spatial distribution of  $W_P$ ,  $W_C$ , ~~WRE~~WRR, AOD, and extent of raining shallow cumulus cloud objects is analyzed by binning them to a  $2.5^\circ \times 2.5^\circ$  global grid.

Figure 1a shows the spatial distribution of  $W_P$  over the global ocean basins, with  $W_P$  increasing equatorward. This is consistent with prior literature that found raining shallow cumulus are most frequent within the tropics (e.g. Smalley and Rapp, 2020).  $W_P$  is largest near the Inter-Tropical Convergence Zone (ITCZ), South Pacific Convergence Zone (SPCZ), and tropical warm pool, with values exceeding  $45 \text{ g m}^{-2}$ . Deep convection is more frequent here (e.g. Waliser and Gautier, 1993), so some objects may be transitioning from raining shallow cumulus to deeper convection. The results likely include a mix of frequently

occurring tropical raining shallow cumulus and the early stages of developing deep convection possibly resulting in large  $W_p$  over the tropics.

195 Spatial patterns in  $W_C$  (Figure 1b) within the tropics generally follow  $W_p$ , with values ranging between  $110 \text{ g m}^{-2}$  and  $150 \text{ g m}^{-2}$  in the tropics. ~~Considering the tropics are more humid than the mid-latitude and polar regions~~We find that relative humidity generally decreases from median values near 90% in the tropics to median values near 80% north or south into the midlatitudes (not shown), this is consistent with modeling studies that found less cloud water evaporates away in wetter environments (e.g. Hernandez-Deckers and Sherwood, 2018)(e.g. Tian and Kuang, 2016). Considering boundary layer depth  
200 scales with SST (e.g. Wood and Bretherton, 2004b), the boundary layer is generally deeper over the tropical oceans than the sub-tropical oceans. This supports deeper clouds (e.g. Short and Nakamura, 2000; Rauber et al., 2007; Smalley and Rapp, 2020) and could also help explain why  $W_C$  and  $W_P$  are largest in the tropics.

Figure 1c shows the spatial patterns in ~~WRE-WRR~~ follow spatial patterns in  $W_p$ , with values increasing equatorward. Shallow cumulus cloud object ~~WRE-WRR~~ is largest within the ITCZ, SPCZ, and tropical warm pool, with values  $> 0.35$ . This  
205 is consistent with Lau and Wu (2003), who found precipitation efficiency is positively correlated with SST (e.g. Lau and Wu, 2003), and implies that ~~WRE-WRR~~ is higher in wetter environments.

Patterns in spatial extent shown in Figure 1d are similar to those found by Smalley and Rapp (2020), who used combined CloudSat/CALIPSO to define extent, with extent decreasing from the stratocumulus regions ~~east-west~~ into the trade cumulus regions and north of the trade cumulus and stratocumulus regions into the ITCZ. Interestingly, Figure 1c shows ~~WRE-WRR~~  
210 also peaks in the southeast Pacific stratocumulus region, implying that ~~WRE-WRR~~ is high in regions with relatively low SST. However, Figure 1e shows that fewer than 40 shallow cumulus objects are observed in a given gridbox over this region in a four-year period, reducing confidence in ~~WRE-WRR~~ here. Together, Figures 1c and 1d indicate that the relationship between ~~WRE-WRR~~ and extent is complicated and potentially depends on cloud depth (which increases in the tropics) and on environmental conditions including ~~environmental moisture RH~~ and aerosol loading.

215 To determine how ~~WRE-WRR~~ depends on cloud size, Figure 2 shows ~~WRE-WRR~~ as a function of cloud object extent. ~~WRE~~  
Note, we estimate the uncertainty in median WRR at any given extent by bootstrapping WRR at a given extent 10,000 times with replacement. Error in WRR median is then classified as  $\pm$  one standard deviation of the bootstrapped sample distribution of median values. Similar error estimates are shown in Figures 3-5 later in this section. ~~WRR~~ follows a double power-law relationship, with ~~WRE-WRR~~  $< 0.25$  for cloud objects  $< 8.3\text{-}8.4 \text{ km}$  and approaching  $0.3\text{-}0.30$  for cloud objects  $> 8.3\text{-}8.4$   
220 km. There is also very little spread in median WRR at a given extent which gives us confidence that this relationship is real. Similar to these results, earlier studies have shown a double power-law distribution in shallow cumulus size (e.g. Benner and Curry, 1998; Trivej and Stevens, 2010), which will be discussed in further detail later.

To address the impact of ~~environmental moisture RH~~ and cloud depth on ~~WREWRR~~, Figure 3 shows the relationship between ~~WRE-WRR~~ and cloud object extent conditioned using cloud-top height and  ~~$< 3 \text{ km}$  relative humidity. Holding environmental~~  
225 ~~moisture constant, WRE RH at or below 850-mb. Holding RH constant, WRR~~ depends strongly on cloud-top height with ~~WRE-WRR~~ nearly doubling for each 0.5 km increase in cloud top height for a given extent in the most humid environments. For a given RH and top height, there is also an increase in ~~WRE-WRR~~ with extent. Holding top height constant, there is also

an increase in ~~WRE with increasing environmental moisture; however, increases in WRE~~ WRR with increasing RH, with no overlap in median WRR error at a given extent or RH. However, increases in WRR are dominated by changing cloud size  
230 (depth and extent).

To support the hypothesis that larger shallow cumulus are able to sustain a larger droplet field within their cores to increase the precipitation efficiency, the variation in the VGZ across individual cloud objects is examined. We expect that VGZ will be a larger negative value near cloud center than cloud ~~edge~~, especially as cloud size increases. As an example, Figure 4a shows the change in median  $VGZ_{CP}$  to  $VGZ_{EP}$  for cloud objects with an extent of ~~10.2~~ 8.4 km. VGZ decreases from ~~10~~ -3.48 dBZ  
235  $km^{-1}$  at cloud object edge to ~~approximately -20~~ -20.3 dBZ  $km^{-1}$  at cloud object center. ~~This demonstrates that larger droplets are~~ Given the relationship between reflectivity and drop size, a negative  $VGZ_{CP}$  implies that drop growth is occurring from near cloud top to near cloud base close to cloud object center, suggesting that larger droplets may be present near cloud base near cloud object center compared to the edge. ~~This~~ To directly analyze drop size near cloud base, Figure 4b shows the spread in median near base reflectivity for cloud objects with an extent of 8.4 km. Figure 4b confirms that cloud drops are largest  
240 near cloud object center, with a median reflectivity of -5.28 dBZ. Reflectivity values, and subsequent drop sizes, then decrease moving from cloud object center to cloud object edge, with edge values of -17.96 dBZ. Figure 4a coupled with 4b implies, at least for extents of ~~10.5~~ 8.4 km, drops grow larger near cloud object centers and may be more protected from mixing.

Figure ~~4b-c~~ shows the relationship between  $VGZ_{CP}$  and  $VGZ_{EP}$  as a function of extent and top height. For a constant cloud-top height,  $VGZ_{CP}$  again follows a double power-law distribution. Specifically, the magnitude of the  $VGZ_{CP}$  rapidly  
245 increases from approximately 10 dBZ  $km^{-1}$  to 20 dBZ  $km^{-1}$  as extent approaches ~~8.3~~ 8.4 km, while it plateaus around 20 dBZ  $km^{-1}$  for extents  $> 8.3$  8.4 km. Conversely,  $VGZ_{EP}$  decreases in magnitude, approaching 0 dBZ  $km^{-1}$  for the largest cloud object extents. However, it does not decrease as fast as  $VGZ_{CP}$ , implying that the change in vertical reflectivity gradient in the center of cloud is driving changes in differences from center to edge. Figure ~~4b-c~~ also shows that the change in  $VGZ_{CP}$  depends on cloud-top height for extents  $> 5.6$  km, with larger magnitudes for the tallest clouds. ~~This is~~  
250 Narrowing this down to the possible influence of entrainment on cloud object updrafts from cloud edge to center, this is also consistent with previous modeling studies that found larger shallow cumulus cloud cores are more insulated from entrainment (e.g. Burnet and Brenguier, 2010; Hernandez-Deckers and Sherwood, 2018), resulting in larger droplets (e.g. Moser and Lasher-Trapp, 2017) (e.g. Burnet and Brenguier, 2010; Tian and Kuang, 2016), a more adiabatic cloud core of developing cumulus as shown in Figure 2 from Moser and Lasher-Trapp (2017), and a higher probability of rainfall (e.g. Smalley and Rapp, 2020) in observations.

To determine how  $VGZ_{CP}$  influences the relationship between ~~WRE~~ WRR and extent, Figure ~~4e~~ shows WRE ~~d~~ shows WRR as a function of extent conditioned by top height and  $VGZ_{CP}$ , with ~~WRE~~ WRR increasing as the magnitude of  $VGZ_{CP}$  increases; however, changes in WRR are not distinct when the magnitude of  $VGZ_{CP}$  is larger than -15 dBZ  $km^{-1}$  for extents  $< 7$  km. This, coupled with Figure ~~4bc~~, illustrates that as shallow cumulus grow deeper and wider, drops at the center of the cloud can  
260 grow larger and scavenge more available cloud water. This is consistent with larger shallow cumulus being more efficient at producing rainfall, perhaps in part because they are less influenced by environmental mixing.

Until this point, this paper has focused on how cloud size and ~~environmental moisture impacts WRR~~ impacts WRR. However, it is also understood that aerosol concentrations influence both the number and size of droplets within a cloud, with larger aerosol concentrations resulting in a greater number of smaller droplets (e.g. Twomey, 1974; Albrecht, 1989). As a result, we hypothesize increasing aerosol concentrations, which vary regionally (Figure 1f), increase the ratio of cloud droplets to rain drops, thus reducing ~~WRR~~ WRR.

Figure 5a shows the relationship between ~~WRR~~ WRR and AOD, conditioned by top height. On first glance, it appears that ~~WRR~~ WRR increases as a function of AOD, which contradicts the expectation of a shift in drop size distribution towards fewer large drops to initiate collision-coalescence which would reduce the amount of cloud water converted to rain water. However, disentangling aerosol-cloud interactions from other meteorological variables is quite difficult, as increasing aerosol concentrations are often correlated with other environmental variables (e.g. Koren et al., 2014).

Given the strong dependence of ~~WRR~~ WRR on top height, we further examine the relationship between AOD and top height (Figure 5b), conditioned by extent. The curves shown in Figure 5a look similar to those shown in Figure 5b, suggesting the positive correlation between aerosols and top height are responsible for the observed relationship between AOD and ~~WRR~~ WRR. Indeed, Figure 5c further supports this assertion. When conditioned by top height, ~~WRR~~ WRR shows little dependence on AOD, and suggests that the conversion from  $W_C$  to  $W_P$  is more sensitive to cloud depth than aerosols. While these results seem counterintuitive, this analysis examines clouds in which precipitation has been detected. ~~Examination of Figure 5d shows the likelihood of precipitation shows the expected decrease with increasing AOD (not shown)~~ rain occurrence at a given AOD determined by the ratio of raining cloud objects to the total number of cloud objects. As expected, Figure 5d shows that the likelihood of rain decreases as AOD increases, with rain likelihood of about 50% in the cleanest environments decreasing to about 40% for an AOD approaching 0.75. These results imply that once the condensation-coalescence is initiated, aerosol loading has a smaller impact on the conversion of cloud water to rain than other cloud or environmental characteristics.

#### 4 Limitations of analysis and observations

This study has emphasized the potential for the decreasing impact of entrainment on cloud cores, resulting in higher WRR, as cloud size increases; however, it is important to point out other factors related to cloud size that may also impact WRR. Figure 3 shows WRR is higher when cloud objects are taller, which may be simply because we are sampling more mature clouds that have had more time for the collision-coalescence process to result in rain formation. Deeper shallow cumulus not only live longer which would give cloud droplets more time to grow to raindrop size (e.g. Burnet and Brenguier, 2010), but they are more likely to have more intense updrafts which could result in more water vapor being transported to higher altitudes within a cloud. Stronger updrafts are then more likely to be able to suspend cloud droplets higher in the cloud for longer periods of time which allows them to grow larger before they begin to fall and collision-coalescence is initiated. Once cloud droplets do begin to fall, they are not only potentially larger but able to collect more droplets over a larger distance than droplets falling through a shallower cloud. This could potentially result in higher WRR, however there is likely a lag between the peaks in cloud water path and rain water path as cloud drops grow to raindrop size in a developing cloud.

295 Earlier modeling studies have also noted that turbulent flow potentially enhances the likelihood of warm rain formation  
(e.g. Brenguier and Chaumat, 2001; Seifert et al., 2010; Wyszogrodzki et al., 2013; Franklin, 2014; Seifert and Onishi, 2016; Chen et al.,  
Seifert et al. (2010) found that turbulence effects are largest near cloud tops in shallow cumulus, which they note is an  
important region for initial rain formation. While these additional processes may impact WRR, the satellite observations used  
300 in this study are instantaneous snapshots in time. We attempted to remove some of these life cycle impacts by binning cloud  
objects by top height. Within a given cloud top height bin, WRR (Figure 3) and the magnitude of  $VGZ_{CP}$  (Figure 4c) still  
increase as a function of extent. While we acknowledge that this cannot fully remove these impacts, these results support the  
idea that processes other than those related to cloud lifetime, like lateral entrainment, may also influence the WRR of shallow  
cumulus of different horizontal sizes.

It is surprising that this study identifies shallow cumulus cloud objects larger than 10 km. This suggests that some stratocumulus  
305 are not being filtered out of this dataset by our LTS threshold. However, a majority of cloud objects that we identify have extents  
below 10 km. This is consistent with Figure 1e which shows that a majority of cloud objects occur over regions generally  
associated with shallow cumulus. To further test this, we performed the same analysis over the south pacific trade region but  
excluded the southeast stratocumulus region, and we still find few large cloud objects with our overall results and interpretation  
not changing. This suggests that predominant type of entrainment impacting these cloud objects would be lateral entrainment  
310 at cloud edges (see review by de Rooy et al., 2013), and that these are indeed shallow cumulus.

At the small end of the shallow cumulus horizontal size spectrum, CloudSat is limited to observing cloud objects no smaller  
than 1.4 x 1.8 km. Given prior ground observational studies, it is likely that there is a significant population of shallow  
cumulus cloud objects not identified by our study (e.g. Kollias et al., 2003; Mieslinger et al., 2019) due to non-uniform beam  
filling effects. Battaglia et al. (2020) noted that this results in an underestimation of path integrated attenuation, potentially  
315 introducing error into the retrieval of  $W_p$ . Unfortunately, this limitation is unavoidable given CloudSat's horizontal resolution.

## 5 Summary and Discussion

This study uses the methodology described by Smalley and Rapp (2020) to classify a large global shallow cumulus cloud  
object dataset from CloudSat and determine the relationship between  $WRE_{WRR}$ , cloud extent, ~~environmental moisture~~ $RH$ ,  
and aerosol loading. We find that  $WRE_{WRR}$  increases as a function of cloud size (top height and extent) and ~~environmental~~  
320 ~~moisture~~ $RH$ . Benner and Curry (1998) found a double-power law distribution in shallow cumulus thickness as a function of  
cloud diameter, and Trivej and Stevens (2010) hypothesized that the shift from one power-law distribution to another results  
from small shallow cumulus that can rapidly grow in size until reaching the trade inversion. We find a similar relationship  
between  $WRE_{WRR}$  and extent, showing that one distribution exists with  $WRE_{WRR}$  increasing faster for extents < ~~8.3~~ $8.4$   
km then slowly increasing above this breakpoint. Trivej and Stevens (2010) also found that environmental factors, particularly  
325 ~~environmental moisture~~ $RH$ , become important once cloud-top height reaches the trade inversion. Our results show that  $WRE_{WRR}$   
 $WRR$  is most sensitive to ~~environmental moisture~~ $RH$  above an extent of ~~8.3~~ $8.4$  km, which we assume represents the average  
extent where cloud objects reach the trade inversion.

Unexpectedly, we find that for a fixed cloud depth, ~~WRE-WRR~~ is fairly insensitive to AOD. One explanation may be that, although high AOD values do occur over the global ocean basins, the majority of cloud objects being sampled still form in relatively clean air, so the minority of cloud objects occurring over polluted regions have a small impact on the overall statistics. Another explanation may be that this analysis only includes precipitating clouds, so once collision-coalescence is initiated, the amount of cloud water converted to rain water is less influenced by aerosol concentrations.

Past studies conclude that precipitation efficiency increases as SST increases (Lau and Wu, 2003; Bailey et al., 2015; Lutsko and Cronin, 2018). Considering warmer SSTs tend to result in deeper clouds (e.g. Wood and Bretherton, 2004a) and more humid environments (e.g. Chen and Liu, 2016), it is reasonable to expect that ~~WRE-WRR~~ would increase in response (e.g. Lau and Wu, 2003). Our results show that ~~WRE-WRR~~ is highest near the equator where SSTs are warmest. However, the general relationship between cloud size (depth and extent), ~~environmental moisture, and WRE suggests that WRE-RH, and WRR suggests that WRR~~ is more sensitive to cloud size than ~~environmental moisture~~RH. To directly address the SST dependence, Figure 6 shows the frequency distribution of extents and the median ~~WRE-WRR~~, both as a function of cloud-top height and SST. For a given cloud-top height, ~~WRE-WRR~~ does increase as a function of SST. However, for a fixed SST, ~~WRE-WRR~~ also increases as extent increases. Additionally, Figure 6 shows that the frequency distribution of cloud object sizes shifts toward more frequent larger extents with increasing SST. Together, these suggest that increasing ~~WRE-WRR~~ with SST shown in past studies not only results from the deepening clouds but also the shift towards more frequent larger clouds.

Prior literature has shown that modeled shallow cumulus cores become more adiabatic as they grow larger (Moser and Lasher-Trapp, 2017), potentially resulting in larger drops. Figure 6 and our analysis of the relationship between VGZCP, extent, and ~~WRE-WRR~~ suggest drop growth is being enhanced near the base at the center of larger cloud objects, potentially resulting in more cloud water being scavenged by larger droplets and more efficient autoconversion and accretion processes. Most climate models parameterize autoconversion and accretion as functions of cloud and precipitation properties (e.g. Lohmann and Roeckner, 1996; Liu and Daum, 2004; Morrison et al., 2005; Lim and Hong, 2010; Lee and Baik, 2017), but recently enhancement factors that depend on variations and covariations in WC and WP have been introduced to correct for biases due to subgrid-scale  $W_c$  and  $W_p$  inhomogeneity (e.g. Lebsock et al., 2013; Boutle et al., 2014; Witte et al., 2019). Presumably, the dependence of these enhancement factors on  $W_c$  variability would capture the increase in ~~WRE-WRR~~ with cloud depth shown here, however it is unclear if these enhancement factors based on the variance in  $W_c$  and  $W_p$  capture the effects of cloud extent on WC and WP, and subsequently ~~WRE-WRR~~. Our dataset provides an opportunity for a future analysis that could focus on investigating the relationship between subgrid-scale variability in WC, WP, ~~WRE-WRR~~, and extent, which could help improve our understanding and simulation of precipitating shallow cloud processes in climate models.

*Data availability.* All CloudSat/MODIS data products used in this analysis were acquired from the CloudSat Data Processing Center and can be accessed at <http://www.cloudsat.cira.colostate.edu>.

360 *Code and data availability.* Please contact the authors for access to any dataset created by the analysis and/or the code used to process the CloudSat/MODIS data..

*Author contributions.* Kevin Smalley performed the analysis. While, Kevin Smalley and Anita Rapp wrote and edited this manuscript.

*Competing interests.* The authors declare they have no conflicts of interest.

*Acknowledgements.* This research was supported by NASA grant NNX14AO72G.

## References

- 365 Abel, S. J. and Shipway, B. J.: A comparison of cloud-resolving model simulations of trade wind cumulus with aircraft observations taken during RICO, *Quarterly Journal of the Royal Meteorological Society*, 133, 781–794, <https://doi.org/https://doi.org/10.1002/qj.55>, <https://rmets.onlinelibrary.wiley.com/doi/abs/10.1002/qj.55>, 2007.
- Albrecht, B. A.: Aerosols, Cloud Microphysics, and Fractional Cloudiness, *Science*, 245, 1227–1230, <https://doi.org/10.1126/science.245.4923.1227>, <https://science.sciencemag.org/content/245/4923/1227>, 1989.
- 370 Austin, R. T., Heymsfield, A. J., and Stephens, G. L.: Retrieval of ice cloud microphysical parameters using the CloudSat millimeter-wave radar and temperature, *Journal of Geophysical Research: Atmospheres*, 114, <https://doi.org/10.1029/2008JD010049>, <https://agupubs.onlinelibrary.wiley.com/doi/abs/10.1029/2008JD010049>, 2009.
- Bailey, A., Nusbaumer, J., and Noone, D.: Precipitation efficiency derived from isotope ratios in water vapor distinguishes dynamical and microphysical influences on subtropical atmospheric constituents, *Journal of Geophysical Research: Atmospheres*, 120, 9119–9137, <https://doi.org/10.1002/2015JD023403>, <https://agupubs.onlinelibrary.wiley.com/doi/abs/10.1002/2015JD023403>, 2015.
- 375 Battaglia, A., Kollias, P., Dhillon, R., Lamer, K., Khairoutdinov, M., and Watters, D.: Mind the gap – Part 2: Improving quantitative estimates of cloud and rain water path in oceanic warm rain using spaceborne radars, *Atmospheric Measurement Techniques*, 13, 4865–4883, <https://doi.org/10.5194/amt-13-4865-2020>, <https://amt.copernicus.org/articles/13/4865/2020/>, 2020.
- Benner, T. C. and Curry, J. A.: Characteristics of small tropical cumulus clouds and their impact on the environment, *Journal of Geophysical Research: Atmospheres*, 103, 28 753–28 767, <https://doi.org/10.1029/98JD02579>, <https://agupubs.onlinelibrary.wiley.com/doi/abs/10.1029/98JD02579>, 1998.
- 380 Blyth, A. M., Lowenstein, J. H., Huang, Y., Cui, Z., Davies, S., and Carslaw, K. S.: The production of warm rain in shallow maritime cumulus clouds, *Quarterly Journal of the Royal Meteorological Society*, 139, 20–31, <https://doi.org/https://doi.org/10.1002/qj.1972>, <https://rmets.onlinelibrary.wiley.com/doi/abs/10.1002/qj.1972>, 2013.
- 385 Bony, S. and Dufresne, J.-L.: Marine boundary layer clouds at the heart of tropical cloud feedback uncertainties in climate models, *Geophysical Research Letters*, 32, <https://doi.org/10.1029/2005GL023851>, <https://agupubs.onlinelibrary.wiley.com/doi/abs/10.1029/2005GL023851>, 2005.
- Boutle, I. A., Abel, S. J., Hill, P. G., and Morcrette, C. J.: Spatial variability of liquid cloud and rain: observations and microphysical effects, *Quarterly Journal of the Royal Meteorological Society*, 140, 583–594, <https://doi.org/10.1002/qj.2140>, <https://rmets.onlinelibrary.wiley.com/doi/abs/10.1002/qj.2140>, 2014.
- 390 Brenguier, J.-L. and Chaumat, L.: Droplet Spectra Broadening in Cumulus Clouds. Part I: Broadening in Adiabatic Cores, *Journal of the Atmospheric Sciences*, 58, 628–641, [https://doi.org/10.1175/1520-0469\(2001\)058<0628:DSBICC>2.0.CO;2](https://doi.org/10.1175/1520-0469(2001)058<0628:DSBICC>2.0.CO;2), [https://doi.org/10.1175/1520-0469\(2001\)058<0628:DSBICC>2.0.CO;2](https://doi.org/10.1175/1520-0469(2001)058<0628:DSBICC>2.0.CO;2), 2001.
- Bretherton, C. S., McCaa, J. R., and Grenier, H.: A New Parameterization for Shallow Cumulus Convection and Its Application to Marine Subtropical Cloud-Topped Boundary Layers. Part I: Description and 1D Results, *Monthly Weather Review*, 132, 864–882, [https://doi.org/10.1175/1520-0493\(2004\)132<0864:ANPFSC>2.0.CO;2](https://doi.org/10.1175/1520-0493(2004)132<0864:ANPFSC>2.0.CO;2), [https://doi.org/10.1175/1520-0493\(2004\)132<0864:ANPFSC>2.0.CO;2](https://doi.org/10.1175/1520-0493(2004)132<0864:ANPFSC>2.0.CO;2), 2004.
- 395 Burnet, F. and Brenguier, J.-L.: The onset of precipitation in warm cumulus clouds: An observational case-study, *Quarterly Journal of the Royal Meteorological Society*, pp. n/a–n/a, <https://doi.org/10.1002/qj.552>, <https://doi.org/10.1002%2Fqj.552>, 2010.

- 400 Chen, B. and Liu, C.: Warm Organized Rain Systems over the Tropical Eastern Pacific, *Journal of Climate*, 29, 3403–3422, <https://doi.org/10.1175/jcli-d-15-0177.1>, <https://doi.org/10.1175%2Fjcli-d-15-0177.1>, 2016.
- Chen, S., Yau, M. K., and Bartello, P.: Turbulence Effects of Collision Efficiency and Broadening of Droplet Size Distribution in Cumulus Clouds, *Journal of the Atmospheric Sciences*, 75, 203–217, <https://doi.org/10.1175/JAS-D-17-0123.1>, <https://doi.org/10.1175/JAS-D-17-0123.1>, 2018.
- 405 Cho, H.-M., Zhang, Z., Meyer, K., Lebsock, M., Platnick, S., Ackerman, A. S., Di Girolamo, L., C.-Labonnote, L., Cornet, C., Riedi, J., and Holz, R. E.: Frequency and causes of failed MODIS cloud property retrievals for liquid phase clouds over global oceans, *Journal of Geophysical Research: Atmospheres*, 120, 4132–4154, <https://doi.org/https://doi.org/10.1002/2015JD023161>, <https://agupubs.onlinelibrary.wiley.com/doi/abs/10.1002/2015JD023161>, 2015.
- Chong, M. and Hauser, D.: A Tropical Squall Line Observed during the COPT 81 Experiment in West Africa. Part II: Water Budget, *Monthly Weather Review*, 117, 728–744, [https://doi.org/10.1175/1520-0493\(1989\)117<0728:ATSLOD>2.0.CO;2](https://doi.org/10.1175/1520-0493(1989)117<0728:ATSLOD>2.0.CO;2), [https://doi.org/10.1175/1520-0493\(1989\)117<0728:ATSLOD>2.0.CO;2](https://doi.org/10.1175/1520-0493(1989)117<0728:ATSLOD>2.0.CO;2), 1989.
- 410 Christensen, M. W., Stephens, G. L., and Lebsock, M. D.: Exposing biases in retrieved low cloud properties from CloudSat: A guide for evaluating observations and climate data, *Journal of Geophysical Research: Atmospheres*, 118, 12,120–12,131, <https://doi.org/10.1002/2013JD020224>, <https://agupubs.onlinelibrary.wiley.com/doi/abs/10.1002/2013JD020224>, 2013.
- 415 Cronk, H. and Partain, P.: CloudSat ECMWF-AUX Auxillary Data Product Process Description and Interface Control Document, Tech. rep., Colorado State University, 2017.
- Cronk, H. and Partain, P.: CloudSat MOD06-AUX Auxiliary Data Process Description and Interface Control Document, Tech. rep., Colorado State University, 2018.
- Dagan, G., Koren, I., Altaratz, O., and Heiblum, R. H.: Aerosol effect on the evolution of the thermodynamic properties of warm convective cloud fields, *Scientific Reports*, 6, <https://doi.org/10.1038/srep38769>, <https://doi.org/10.1038%2Fsrep38769>, 2016.
- 420 de Rooy, W. C., Bechtold, P., Fröhlich, K., Hohenegger, C., Jonker, H., Mironov, D., Pier Siebesma, A., Teixeira, J., and Yano, J.-I.: Entrainment and detrainment in cumulus convection: an overview, *Quarterly Journal of the Royal Meteorological Society*, 139, 1–19, <https://doi.org/https://doi.org/10.1002/qj.1959>, <https://rmets.onlinelibrary.wiley.com/doi/abs/10.1002/qj.1959>, 2013.
- Del Genio, A. D., Kovari, W., Yao, M.-S., and Jonas, J.: Cumulus Microphysics and Climate Sensitivity, *Journal of Climate*, 18, 2376–2387, <https://doi.org/10.1175/JCLI3413.1>, <https://doi.org/10.1175/JCLI3413.1>, 2005.
- 425 Dufresne, J.-L. and Bony, S.: An Assessment of the Primary Sources of Spread of Global Warming Estimates from Coupled Atmosphere–Ocean Models, *Journal of Climate*, 21, 5135–5144, <https://doi.org/10.1175/2008JCLI2239.1>, <https://doi.org/10.1175/2008JCLI2239.1>, 2008.
- Franklin, C. N.: The effects of turbulent collision–coalescence on precipitation formation and precipitation-dynamical feedbacks in simulations of stratocumulus and shallow cumulus convection, *Atmospheric Chemistry and Physics*, 14, 6557–6570, <https://doi.org/10.5194/acp-14-6557-2014>, <https://acp.copernicus.org/articles/14/6557/2014/>, 2014.
- 430 Gerber, H. E., Frick, G. M., Jensen, J. B., and Hudson, J. G.: Entrainment, Mixing, and Microphysics in Trade-Wind Cumulus, *Journal of the Meteorological Society of Japan. Ser. II*, 86A, 87–106, <https://doi.org/10.2151/jmsj.86A.87>, 2008.
- Haynes, J. M., LEcuyer, T. S., Stephens, G. L., Miller, S. D., Mitrescu, C., Wood, N. B., and Tanelli, S.: Rainfall retrieval over the ocean with spaceborne W-band radar, *Journal of Geophysical Research*, 114, <https://doi.org/10.1029/2008jd009973>, <https://doi.org/10.1029%2F2008jd009973>, 2009.
- 435

- Hernandez-Deckers, D. and Sherwood, S. C.: On the Role of Entrainment in the Fate of Cumulus Thermals, *Journal of the Atmospheric Sciences*, 75, 3911–3924, <https://doi.org/10.1175/jas-d-18-0077.1>, <https://doi.org/10.1175%2Fjas-d-18-0077.1>, 2018.
- 440 Heus, T. and Jonker, H. J. J.: Subsiding Shells around Shallow Cumulus Clouds, *Journal of the Atmospheric Sciences*, 65, 1003–1018, <https://doi.org/10.1175/2007jas2322.1>, <https://doi.org/10.1175%2F2007jas2322.1>, 2008.
- Hoffmann, F., Noh, Y., and Raasch, S.: The Route to Raindrop Formation in a Shallow Cumulus Cloud Simulated by a Lagrangian Cloud Model, *Journal of the Atmospheric Sciences*, 74, 2125–2142, <https://doi.org/10.1175/JAS-D-16-0220.1>, <https://doi.org/10.1175/JAS-D-16-0220.1>, 2017.
- 445 Jiang, H. and Feingold, G.: Effect of aerosol on warm convective clouds: Aerosol-cloud-surface flux feedbacks in a new coupled large eddy model, *Journal of Geophysical Research: Atmospheres*, 111, <https://doi.org/10.1029/2005JD006138>, <https://agupubs.onlinelibrary.wiley.com/doi/abs/10.1029/2005JD006138>, 2006.
- Jolivet, D. and Feijt, A. J.: Quantification of the accuracy of liquid water path fields derived from NOAA 16 advanced very high resolution radiometer over three ground stations using microwave radiometers, *Journal of Geophysical Research: Atmospheres*, 110, <https://doi.org/https://doi.org/10.1029/2004JD005205>, <https://agupubs.onlinelibrary.wiley.com/doi/abs/10.1029/2004JD005205>, 2005.
- 450 Jung, E., Albrecht, B. A., Feingold, G., Jonsson, H. H., Chuang, P., and Donaher, S. L.: Aerosols, clouds, and precipitation in the North Atlantic trades observed during the Barbados aerosol cloud experiment – Part 1: Distributions and variability, *Atmospheric Chemistry and Physics*, 16, 8643–8666, <https://doi.org/10.5194/acp-16-8643-2016>, <https://doi.org/10.5194%2FACP-16-8643-2016>, 2016a.
- Jung, E., Albrecht, B. A., Sorooshian, A., Zuidema, P., and Jonsson, H. H.: Precipitation susceptibility in marine stratocumulus and shallow cumulus from airborne measurements, *Atmospheric Chemistry and Physics*, 16, 11395–11413, <https://doi.org/10.5194/acp-16-11395-2016>, <https://doi.org/10.5194%2FACP-16-11395-2016>, 2016b.
- 455 Kollias, P., Albrecht, B. A., and Marks Jr., F. D.: Cloud radar observations of vertical drafts and microphysics in convective rain, *Journal of Geophysical Research: Atmospheres*, 108, <https://doi.org/10.1029/2001JD002033>, <https://agupubs.onlinelibrary.wiley.com/doi/abs/10.1029/2001JD002033>, 2003.
- Koren, I., Dagan, G., and Altaratz, O.: From aerosol-limited to invigoration of warm convective clouds, *Science*, 344, 1143–1146, <https://doi.org/10.1126/science.1252595>, <https://science.sciencemag.org/content/344/6188/1143>, 2014.
- 460 Korolev, A., Khain, A., Pinsky, M., and French, J.: Theoretical study of mixing in liquid clouds – Part 1: Classical concepts, *Atmospheric Chemistry and Physics*, 16, 9235–9254, <https://doi.org/10.5194/acp-16-9235-2016>, <https://doi.org/10.5194%2FACP-16-9235-2016>, 2016.
- Lamer, K., Kollias, P., Battaglia, A., and Preval, S.: Mind the gap – Part 1: Accurately locating warm marine boundary layer clouds and precipitation using spaceborne radars, *Atmospheric Measurement Techniques*, 13, 2363–2379, <https://doi.org/10.5194/amt-13-2363-2020>, <https://amt.copernicus.org/articles/13/2363/2020/>, 2020.
- 465 Lau, K. M. and Wu, H. T.: Warm rain processes over tropical oceans and climate implications, *Geophysical Research Letters*, 30, <https://doi.org/10.1029/2003GL018567>, <https://agupubs.onlinelibrary.wiley.com/doi/abs/10.1029/2003GL018567>, 2003.
- Lebsock, M.: Level 2C RAIN-PROFILE Product Process Description and Interface Control Document, Tech. Rep. D-20308, Jet Propulsion Laboratory, California Institute of Technology, Pasadena, California, 2018.
- 470 Lebsock, M. and Su, H.: Application of active spaceborne remote sensing for understanding biases between passive cloud water path retrievals, *Journal of Geophysical Research: Atmospheres*, 119, 8962–8979, <https://doi.org/10.1002/2014JD021568>, <https://agupubs.onlinelibrary.wiley.com/doi/abs/10.1002/2014JD021568>, 2014.

- Lebsock, M., Morrison, H., and Gettelman, A.: Microphysical implications of cloud-precipitation covariance derived from satellite remote sensing, *Journal of Geophysical Research: Atmospheres*, 118, 6521–6533, <https://doi.org/10.1002/jgrd.50347>, <https://agupubs.onlinelibrary.wiley.com/doi/abs/10.1002/jgrd.50347>, 2013.
- 475 Lebsock, M. D. and L'Ecuyer, T. S.: The retrieval of warm rain from CloudSat, *Journal of Geophysical Research: Atmospheres*, 116, <https://doi.org/10.1029/2011JD016076>, <https://agupubs.onlinelibrary.wiley.com/doi/abs/10.1029/2011JD016076>, 2011.
- Lebsock, M. D., L'Ecuyer, T. S., and Stephens, G. L.: Detecting the Ratio of Rain and Cloud Water in Low-Latitude Shallow Marine Clouds, *Journal of Applied Meteorology and Climatology*, 50, 419–432, <https://doi.org/10.1175/2010JAMC2494.1>, <https://doi.org/10.1175/2010JAMC2494.1>, 2011.
- 480 L'Ecuyer, T. S. and Stephens, G. L.: An Estimation-Based Precipitation Retrieval Algorithm for Attenuating Radars, *Journal of Applied Meteorology*, 41, 272–285, [https://doi.org/10.1175/1520-0450\(2002\)041<0272:AEBPRA>2.0.CO;2](https://doi.org/10.1175/1520-0450(2002)041<0272:AEBPRA>2.0.CO;2), [https://doi.org/10.1175/1520-0450\(2002\)041<0272:AEBPRA>2.0.CO;2](https://doi.org/10.1175/1520-0450(2002)041<0272:AEBPRA>2.0.CO;2), 2002.
- Lee, H. and Baik, J.-J.: A Physically Based Autoconversion Parameterization, *Journal of the Atmospheric Sciences*, 74, 1599–1616, <https://doi.org/10.1175/JAS-D-16-0207.1>, <https://doi.org/10.1175/JAS-D-16-0207.1>, 2017.
- 485 Lim, K.-S. S. and Hong, S.-Y.: Development of an Effective Double-Moment Cloud Microphysics Scheme with Prognostic Cloud Condensation Nuclei (CCN) for Weather and Climate Models, *Monthly Weather Review*, 138, 1587–1612, <https://doi.org/10.1175/2009MWR2968.1>, <https://doi.org/10.1175/2009MWR2968.1>, 2010.
- Liu, J. and Li, Z.: Significant Underestimation in the Optically Based Estimation of the Aerosol First Indirect Effect Induced by the Aerosol Swelling Effect, *Geophysical Research Letters*, 45, 5690–5699, <https://doi.org/https://doi.org/10.1029/2018GL077679>, <https://agupubs.onlinelibrary.wiley.com/doi/abs/10.1029/2018GL077679>, 2018.
- 490 Liu, Y. and Daum, P. H.: Parameterization of the Autoconversion Process. Part I: Analytical Formulation of the Kessler-Type Parameterizations, *Journal of the Atmospheric Sciences*, 61, 1539–1548, [https://doi.org/10.1175/1520-0469\(2004\)061<1539:POTAPI>2.0.CO;2](https://doi.org/10.1175/1520-0469(2004)061<1539:POTAPI>2.0.CO;2), [https://doi.org/10.1175/1520-0469\(2004\)061<1539:POTAPI>2.0.CO;2](https://doi.org/10.1175/1520-0469(2004)061<1539:POTAPI>2.0.CO;2), 2004.
- 495 Lohmann, U. and Roeckner, E.: Design and performance of a new cloud microphysics scheme developed for the ECHAM general circulation model, *Climate Dynamics*, 12, 557–572, <https://doi.org/10.1007/BF00207939>, <https://doi.org/10.1007/BF00207939>, 1996.
- Lu, C., Liu, Y., Niu, S., and Vogelmann, A. M.: Lateral entrainment rate in shallow cumuli: Dependence on dry air sources and probability density functions, *Geophysical Research Letters*, 39, <https://doi.org/10.1029/2012GL053646>, <https://agupubs.onlinelibrary.wiley.com/doi/abs/10.1029/2012GL053646>, 2012.
- 500 Lutsko, N. J. and Cronin, T. W.: Increase in Precipitation Efficiency With Surface Warming in Radiative-Convective Equilibrium, *Journal of Advances in Modeling Earth Systems*, 10, 2992–3010, <https://doi.org/10.1029/2018MS001482>, <https://agupubs.onlinelibrary.wiley.com/doi/abs/10.1029/2018MS001482>, 2018.
- Marchand, R., Mace, G. G., Ackerman, T., and Stephens, G.: Hydrometeor Detection Using Cloudsat—An Earth-Orbiting 94-GHz Cloud Radar, *Journal of Atmospheric and Oceanic Technology*, 25, 519–533, <https://doi.org/10.1175/2007JTECHA1006.1>, <https://doi.org/10.1175/2007JTECHA1006.1>, 2008.
- 505 Medeiros, B. and Stevens, B.: Revealing differences in GCM representations of low clouds, *Climate Dynamics*, 36, 385–399, <https://doi.org/10.1007/s00382-009-0694-5>, <https://doi.org/10.1007/s00382-009-0694-5>, 2011.
- Michel Flores, J., Bar-Or, R. Z., Bluvshstein, N., Abo-Riziq, A., Kostinski, A., Borrmann, S., Koren, I., Koren, I., and Rudich, Y.: Absorbing aerosols at high relative humidity: linking hygroscopic growth to optical properties, *Atmospheric Chemistry and Physics*, 12, 5511–5521, <https://doi.org/10.5194/acp-12-5511-2012>, <https://acp.copernicus.org/articles/12/5511/2012/>, 2012.
- 510

- Mieslinger, T., Horvath, A., Buehler, S. A., and Sakradzija, M.: The Dependence of Shallow Cumulus Macrophysical Properties on Large-Scale Meteorology as Observed in ASTER Imagery, *Journal of Geophysical Research: Atmospheres*, 124, 11 477–11 505, <https://doi.org/https://doi.org/10.1029/2019JD030768>, <https://agupubs.onlinelibrary.wiley.com/doi/abs/10.1029/2019JD030768>, 2019.
- 515 Minor, H. A., Rauber, R. M., Göke, S., and Di Girolamo, L.: Trade Wind Cloud Evolution Observed by Polarization Radar: Relationship to Giant Condensation Nuclei Concentrations and Cloud Organization, *Journal of the Atmospheric Sciences*, 68, 1075–1096, <https://doi.org/10.1175/2010JAS3675.1>, <https://doi.org/10.1175/2010JAS3675.1>, 2011.
- Mitrescu, C., L'Ecuyer, T., Haynes, J., Miller, S., and Turk, J.: CloudSat Precipitation Profiling Algorithm—Model Description, *Journal of Applied Meteorology and Climatology*, 49, 991–1003, <https://doi.org/10.1175/2009JAMC2181.1>, <https://doi.org/10.1175/2009JAMC2181.1>, 2010.
- 520 Morrison, H., Curry, J. A., and Khvorostyanov, V. I.: A New Double-Moment Microphysics Parameterization for Application in Cloud and Climate Models. Part I: Description, *Journal of the Atmospheric Sciences*, 62, 1665–1677, <https://doi.org/10.1175/JAS3446.1>, <https://doi.org/10.1175/JAS3446.1>, 2005.
- Moser, D. H. and Lasher-Trapp, S.: The Influence of Successive Thermals on Entrainment and Dilution in a Simulated Cumulus Congestus, *Journal of the Atmospheric Sciences*, 74, 375–392, <https://doi.org/10.1175/JAS-D-16-0144.1>, <https://doi.org/10.1175/JAS-D-16-0144.1>, 525 2017.
- Nam, C., Bony, S., Dufresne, J.-L., and Chepfer, H.: The ‘too few, too bright’ tropical low-cloud problem in CMIP5 models, *Geophysical Research Letters*, 39, <https://doi.org/10.1029/2012GL053421>, <https://agupubs.onlinelibrary.wiley.com/doi/abs/10.1029/2012GL053421>, 2012.
- Neubauer, D., Christensen, M. W., Poulsen, C. A., and Lohmann, U.: Unveiling aerosol–cloud interactions – Part 2: Minimising the effects 530 of aerosol swelling and wet scavenging in ECHAM6-HAM2 for comparison to satellite data, *Atmospheric Chemistry and Physics*, 17, 13 165–13 185, <https://doi.org/10.5194/acp-17-13165-2017>, <https://acp.copernicus.org/articles/17/13165/2017/>, 2017.
- Pinsky, M., Khain, A., and Korolev, A.: Theoretical analysis of mixing in liquid clouds – Part 3: Inhomogeneous mixing, *Atmospheric Chemistry and Physics*, 16, 9273–9297, <https://doi.org/10.5194/acp-16-9273-2016>, <https://doi.org/10.5194%2Facp-16-9273-2016>, 2016a.
- Pinsky, M., Khain, A., Korolev, A., and Magaritz-Ronen, L.: Theoretical investigation of mixing in warm clouds – Part 2: Homogeneous 535 mixing, *Atmospheric Chemistry and Physics*, 16, 9255–9272, <https://doi.org/10.5194/acp-16-9255-2016>, <https://doi.org/10.5194%2Facp-16-9255-2016>, 2016b.
- Platnick, S. and Valero, F. P. J.: A Validation of a Satellite Cloud Retrieval during ASTEX, *Journal of the Atmospheric Sciences*, 52, 2985–3001, [https://doi.org/10.1175/1520-0469\(1995\)052<2985:AVOASC>2.0.CO;2](https://doi.org/10.1175/1520-0469(1995)052<2985:AVOASC>2.0.CO;2), [https://doi.org/10.1175/1520-0469\(1995\)052<2985:AVOASC>2.0.CO;2](https://doi.org/10.1175/1520-0469(1995)052<2985:AVOASC>2.0.CO;2), 1995.
- 540 Platnick, S., King, M. D., Ackerman, S. A., Menzel, W. P., Baum, B. A., Riedi, J. C., and Frey, R. A.: The MODIS cloud products: algorithms and examples from Terra, *IEEE Transactions on Geoscience and Remote Sensing*, 41, 459–473, 2003.
- Rauber, R. M., Stevens, B., Ochs, H. T., Knight, C., Albrecht, B. A., Blyth, A. M., Fairall, C. W., Jensen, J. B., Lasher-Trapp, S. G., Mayol-Bracero, O. L., Vali, G., Anderson, J. R., Baker, B. A., Bandy, A. R., Burnet, E., Brenguier, J.-L., Brewer, W. A., Brown, P. R. A., Chuang, R., Cotton, W. R., Girolamo, L. D., Geerts, B., Gerber, H., G $\ddot{a}$ llke, S., Gomes, L., Heikes, B. G., Hudson, J. G., Kollias, 545 P., Lawson, R. R., Krueger, S. K., Lenschow, D. H., Nuijens, L., O'Sullivan, D. W., Rilling, R. A., Rogers, D. C., Siebesma, A. P., Snodgrass, E., Stith, J. L., Thornton, D. C., Tucker, S., Twohy, C. H., and Zuidema, P.: Rain in Shallow Cumulus Over the Ocean: The RICO Campaign, *Bulletin of the American Meteorological Society*, 88, 1912–1928, <https://doi.org/10.1175/bams-88-12-1912>, <https://doi.org/10.1175%2Fbams-88-12-1912>, 2007.

- 550 Rennó, N. O., Emanuel, K. A., and Stone, P. H.: Radiative-convective model with an explicit hydrologic cycle: 1. Formulation and sensitivity to model parameters, *Journal of Geophysical Research: Atmospheres*, 99, 14 429–14 441, <https://doi.org/10.1029/94JD00020>, <https://agupubs.onlinelibrary.wiley.com/doi/abs/10.1029/94JD00020>, 1994.
- Romps, D. M.: An Analytical Model for Tropical Relative Humidity, *Journal of Climate*, 27, 7432–7449, <https://doi.org/10.1175/JCLI-D-14-00255.1>, <https://doi.org/10.1175/JCLI-D-14-00255.1>, 2014.
- 555 Ruiz-Arias, J. A., Dudhia, J., Gueymard, C. A., and Pozo-Vázquez, D.: Assessment of the Level-3 MODIS daily aerosol optical depth in the context of surface solar radiation and numerical weather modeling, *Atmospheric Chemistry and Physics*, 13, 675–692, <https://doi.org/10.5194/acp-13-675-2013>, <https://www.atmos-chem-phys.net/13/675/2013/>, 2013.
- Saleeby, S. M., Herbener, S. R., van den Heever, S. C., and L'Ecuyer, T.: Impacts of Cloud Droplet–Nucleating Aerosols on Shallow Tropical Convection, *Journal of the Atmospheric Sciences*, 72, 1369–1385, <https://doi.org/10.1175/JAS-D-14-0153.1>, <https://doi.org/10.1175/JAS-D-14-0153.1>, 2015.
- 560 Schmeissner, T., Shaw, R. A., Ditas, J., Stratmann, F., Wendisch, M., and Siebert, H.: Turbulent Mixing in Shallow Trade Wind Cumuli: Dependence on Cloud Life Cycle, *Journal of the Atmospheric Sciences*, 72, 1447–1465, <https://doi.org/10.1175/jas-d-14-0230.1>, <https://doi.org/10.1175%2Fjas-d-14-0230.1>, 2015.
- Seethala, C. and Horvath, A.: Global assessment of AMSR-E and MODIS cloud liquid water path retrievals in warm oceanic clouds, *Journal of Geophysical Research: Atmospheres*, 115, <https://doi.org/https://doi.org/10.1029/2009JD012662>, <https://agupubs.onlinelibrary.wiley.com/doi/abs/10.1029/2009JD012662>, 2010.
- 565 Seifert, A. and Onishi, R.: Turbulence effects on warm-rain formation in precipitating shallow convection revisited, *Atmospheric Chemistry and Physics*, 16, 12 127–12 141, <https://doi.org/10.5194/acp-16-12127-2016>, <https://acp.copernicus.org/articles/16/12127/2016/>, 2016.
- Seifert, A., Nuijens, L., and Stevens, B.: Turbulence effects on warm-rain autoconversion in precipitating shallow convection, *Quarterly Journal of the Royal Meteorological Society*, 136, 1753–1762, <https://doi.org/https://doi.org/10.1002/qj.684>, <https://rmets.onlinelibrary.wiley.com/doi/abs/10.1002/qj.684>, 2010.
- 570 Short, D. A. and Nakamura, K.: TRMM Radar Observations of Shallow Precipitation over the Tropical Oceans, *Journal of Climate*, 13, 4107–4124, [https://doi.org/10.1175/1520-0442\(2000\)013<4107:TROOSP>2.0.CO;2](https://doi.org/10.1175/1520-0442(2000)013<4107:TROOSP>2.0.CO;2), [https://doi.org/10.1175/1520-0442\(2000\)013<4107:TROOSP>2.0.CO;2](https://doi.org/10.1175/1520-0442(2000)013<4107:TROOSP>2.0.CO;2), 2000.
- Smalley, K. M. and Rapp, A. D.: The role of cloud size and environmental moisture in shallow cumulus precipitation, *Journal of Applied Meteorology and Climatology*, 0, null, <https://doi.org/10.1175/JAMC-D-19-0145.1>, <https://doi.org/10.1175/JAMC-D-19-0145.1>, 2020.
- Squires, P.: The Microstructure and Colloidal Stability of Warm Clouds, *Tellus*, 10, 256–261, <https://doi.org/10.1111/j.2153-3490.1958.tb02011.x>, <https://onlinelibrary.wiley.com/doi/abs/10.1111/j.2153-3490.1958.tb02011.x>, 1958.
- Stevens, D. E., Ackerman, A. S., and Bretherton, C. S.: Effects of domain size and numerical resolution on the simulation of shallow cumulus convection, *J. Atmos. Sci.*, 59, 3285–3301, [https://doi.org/10.1175/1520-0469\(2002\)0593C32853AEODSAN3E2.0.CO;2](https://doi.org/10.1175/1520-0469(2002)0593C32853AEODSAN3E2.0.CO;2), 2002.
- 580 Su, W., Schuster, G. L., Loeb, N. G., Rogers, R. R., Ferrare, R. A., Hostetler, C. A., Hair, J. W., and Obland, M. D.: Aerosol and cloud interaction observed from high spectral resolution lidar data, *Journal of Geophysical Research: Atmospheres*, 113, <https://doi.org/https://doi.org/10.1029/2008JD010588>, <https://agupubs.onlinelibrary.wiley.com/doi/abs/10.1029/2008JD010588>, 2008.
- Sui, C.-H., Li, X., and Yang, M.-J.: On the Definition of Precipitation Efficiency, *Journal of the Atmospheric Sciences*, 64, 4506–4513, <https://doi.org/10.1175/2007JAS2332.1>, <https://doi.org/10.1175/2007JAS2332.1>, 2007.

- 585 Tanelli, S., Durden, S. L., Im, E., Pak, K. S., Reinke, D. G., Partain, P., Haynes, J. M., and Marchand, R. T.: CloudSat's Cloud Profiling Radar After Two Years in Orbit: Performance, Calibration, and Processing, *IEEE Transactions on Geoscience and Remote Sensing*, 46, 3560–3573, <https://doi.org/10.1109/TGRS.2008.2002030>, 2008.
- Tao, W.-K., Johnson, D., Shie, C.-L., and Simpson, J.: The Atmospheric Energy Budget and Large-Scale Precipitation Efficiency of Convective Systems during TOGA COARE, GATE, SCSMEX, and ARM: Cloud-Resolving Model Simulations, *Journal of the Atmospheric Sciences*, 61, 2405–2423, [https://doi.org/10.1175/1520-0469\(2004\)061<2405:TAEBAL>2.0.CO;2](https://doi.org/10.1175/1520-0469(2004)061<2405:TAEBAL>2.0.CO;2), [https://doi.org/10.1175/1520-0469\(2004\)061<2405:TAEBAL>2.0.CO;2](https://doi.org/10.1175/1520-0469(2004)061<2405:TAEBAL>2.0.CO;2), 2004.
- 590 Tian, Y. and Kuang, Z.: Dependence of entrainment in shallow cumulus convection on vertical velocity and distance to cloud edge, *Geophysical Research Letters*, 43, 4056–4065, <https://doi.org/10.1002/2016gl069005>, <https://doi.org/10.1002%2F2016gl069005>, 2016.
- Tiedtke, M.: A Comprehensive Mass Flux Scheme for Cumulus Parameterization in Large-Scale Models, *Monthly Weather Review*, 117, 1779–1800, [https://doi.org/10.1175/1520-0493\(1989\)117<1779:ACMFSF>2.0.CO;2](https://doi.org/10.1175/1520-0493(1989)117<1779:ACMFSF>2.0.CO;2), [https://doi.org/10.1175/1520-0493\(1989\)117<1779:ACMFSF>2.0.CO;2](https://doi.org/10.1175/1520-0493(1989)117<1779:ACMFSF>2.0.CO;2), 1989.
- 595 Trivej, P. and Stevens, B.: The Echo Size Distribution of Precipitating Shallow Cumuli, *Journal of the Atmospheric Sciences*, 67, 788–804, <https://doi.org/10.1175/2009JAS3178.1>, <https://doi.org/10.1175/2009JAS3178.1>, 2010.
- Twomey, S.: Pollution and the planetary albedo, *Atmospheric Environment*, 8, 1251 – 1256, [https://doi.org/https://doi.org/10.1016/0004-6981\(74\)90004-3](https://doi.org/https://doi.org/10.1016/0004-6981(74)90004-3), <http://www.sciencedirect.com/science/article/pii/0004698174900043>, 1974.
- 600 vanZanten, M. C., Stevens, B., Nuijens, L., Siebesma, A. P., Ackerman, A. S., Burnet, F., Cheng, A., Couvreux, F., Jiang, H., Khairoutdinov, M., Kogan, Y., Lewellen, D. C., Mechem, D., Nakamura, K., Noda, A., Shipway, B. J., Slawinska, J., Wang, S., and Wyszogrodzki, A.: Controls on precipitation and cloudiness in simulations of trade-wind cumulus as observed during RICO, *Journal of Advances in Modeling Earth Systems*, 3, <https://doi.org/https://doi.org/10.1029/2011MS000056>, <https://agupubs.onlinelibrary.wiley.com/doi/abs/10.1029/2011MS000056>, 2011.
- 605 Vial, J., Dufresne, J.-L., and Bony, S.: On the interpretation of inter-model spread in CMIP5 climate sensitivity estimates, *Climate Dynamics*, 41, 3339–3362, <https://doi.org/10.1007/s00382-013-1725-9>, <https://doi.org/10.1007/s00382-013-1725-9>, 2013.
- Waliser, D. E. and Gautier, C.: A Satellite-derived Climatology of the ITCZ, *Journal of Climate*, 6, 2162–2174, [https://doi.org/10.1175/1520-0442\(1993\)006<2162:ASDCOT>2.0.CO;2](https://doi.org/10.1175/1520-0442(1993)006<2162:ASDCOT>2.0.CO;2), [https://doi.org/10.1175/1520-0442\(1993\)006<2162:ASDCOT>2.0.CO;2](https://doi.org/10.1175/1520-0442(1993)006<2162:ASDCOT>2.0.CO;2), 1993.
- 610 Wang, Y., Chen, Y., Fu, Y., and Liu, G.: Identification of precipitation onset based on Cloudsat observations, *Journal of Quantitative Spectroscopy and Radiative Transfer*, 188, 142 – 147, <https://doi.org/https://doi.org/10.1016/j.jqsrt.2016.06.028>, <http://www.sciencedirect.com/science/article/pii/S0022407315301886>, *advances in Atmospheric Light Scattering: Theory and Remote Sensing Techniques*, 2017.
- Watson, C. D., Smith, R. B., and Nugent, A. D.: Processes Controlling Precipitation in Shallow, Orographic, Trade Wind Convection, *Journal of the Atmospheric Sciences*, 72, 3051–3072, <https://doi.org/10.1175/JAS-D-14-0333.1>, <https://doi.org/10.1175/JAS-D-14-0333.1>, 2015.
- 615 Witkowski, M., Vane, D., Livermore, T., Rokey, M., Barthuli, M., Gravseth, I. J., Pieper, B., Rodzinak, A., Silva, S., and Woznick, P.: CloudSat anomaly recovery and operational lessons learned, Tech. rep., Jet Propulsion Laboratory, National Aeronautics and Space Administration, 2012.
- Witte, M. K., Morrison, H., Jensen, J. B., Bansemer, A., and Gettelman, A.: On the Covariability of Cloud and Rain Water as a Function of Length Scale, *Journal of the Atmospheric Sciences*, 76, 2295–2308, <https://doi.org/10.1175/JAS-D-19-0048.1>, <https://doi.org/10.1175/JAS-D-19-0048.1>, 2019.
- 620

- Wood, R. and Bretherton, C. S.: Boundary Layer Depth, Entrainment, and Decoupling in the Cloud-Capped Subtropical and Tropical Marine Boundary Layer, *Journal of Climate*, 17, 3576–3588, [https://doi.org/10.1175/1520-0442\(2004\)017<3576:BLDEAD>2.0.CO;2](https://doi.org/10.1175/1520-0442(2004)017<3576:BLDEAD>2.0.CO;2), [https://doi.org/10.1175/1520-0442\(2004\)017<3576:BLDEAD>2.0.CO;2](https://doi.org/10.1175/1520-0442(2004)017<3576:BLDEAD>2.0.CO;2), 2004a.
- 625 Wood, R. and Bretherton, C. S.: Boundary Layer Depth, Entrainment, and Decoupling in the Cloud-Capped Subtropical and Tropical Marine Boundary Layer, *Journal of Climate*, 17, 3576–3588, [https://doi.org/10.1175/1520-0442\(2004\)017<3576:BLDEAD>2.0.CO;2](https://doi.org/10.1175/1520-0442(2004)017<3576:BLDEAD>2.0.CO;2), [https://doi.org/10.1175/1520-0442\(2004\)017<3576:BLDEAD>2.0.CO;2](https://doi.org/10.1175/1520-0442(2004)017<3576:BLDEAD>2.0.CO;2), 2004b.
- Wyant, M. C., Khairoutdinov, M., and Bretherton, C. S.: Climate sensitivity and cloud response of a GCM with a superparameterization, *Geophysical Research Letters*, 33, <https://doi.org/10.1029/2005GL025464>, <https://agupubs.onlinelibrary.wiley.com/doi/abs/10.1029/2005GL025464>, 2006.
- 630 Wyszogrodzki, A. A., Grabowski, W. W., Wang, L.-P., and Ayala, O.: Turbulent collision-coalescence in maritime shallow convection, *Atmospheric Chemistry and Physics*, 13, 8471–8487, <https://doi.org/10.5194/acp-13-8471-2013>, <https://acp.copernicus.org/articles/13/8471/2013/>, 2013.
- Zhang, G. and McFarlane, N. A.: Sensitivity of climate simulations to the parameterization of cumulus convection in the Canadian climate centre general circulation model, *Atmosphere-Ocean*, 33, 407–446, <https://doi.org/10.1080/07055900.1995.9649539>, <https://doi.org/10.1080/07055900.1995.9649539>, 1995.
- 635 Zhao, M.: An Investigation of the Connections among Convection, Clouds, and Climate Sensitivity in a Global Climate Model, *Journal of Climate*, 27, 1845–1862, <https://doi.org/10.1175/JCLI-D-13-00145.1>, <https://doi.org/10.1175/JCLI-D-13-00145.1>, 2014.

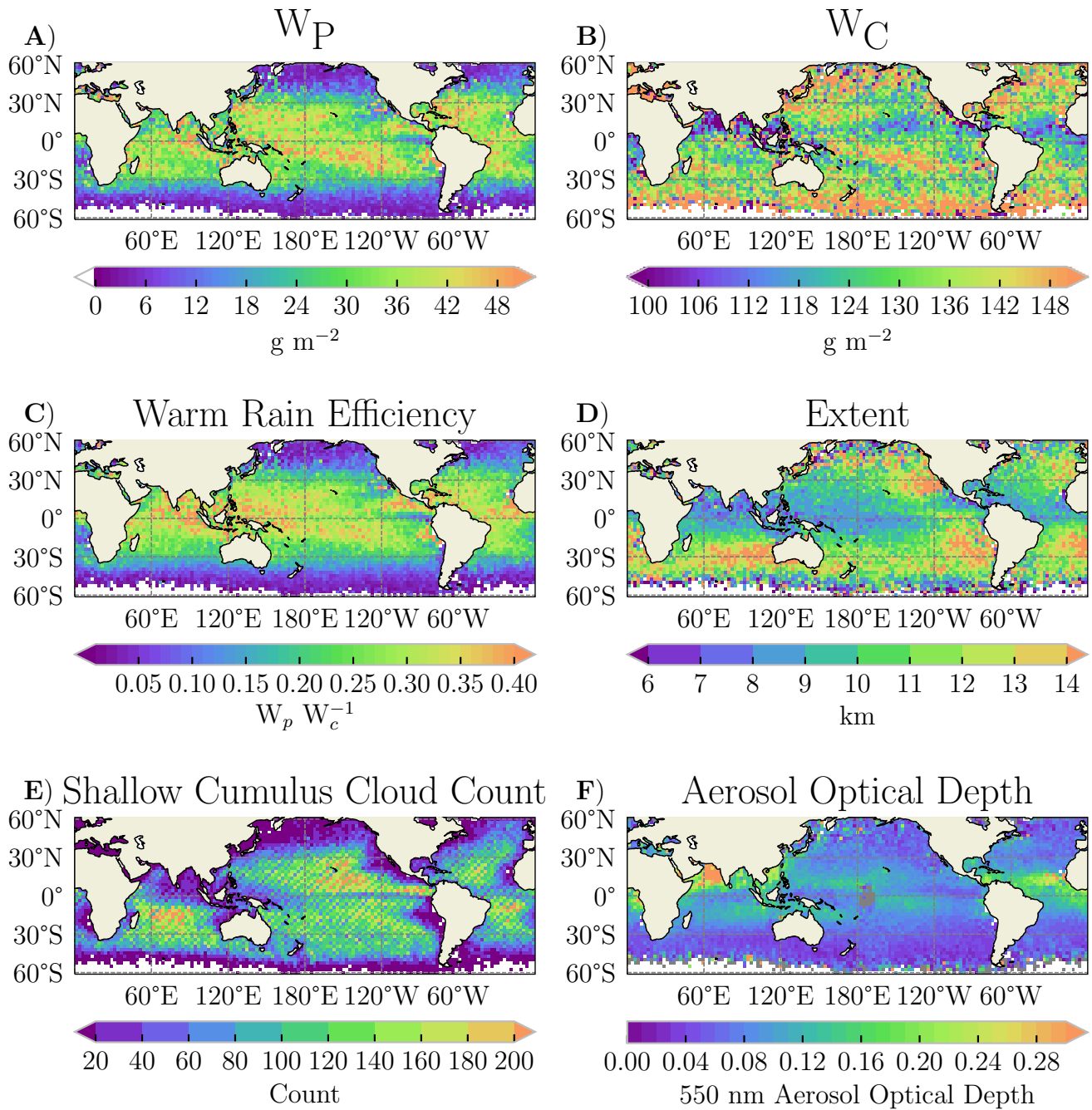


**Figure 1.** The spatial distribution of integrated precipitation water path ( $W_p$ ), cloud water path ( $W_c$ ), warm rain efficiency, extent, number of shallow cumulus cloud objects, and aerosol optical depth are shown in panels A), B), C), D), E), and F) respectively. Cloud objects are binned onto a  $2.5^\circ \times 2.5^\circ$  spatial grid, and any grid box containing no data is white.

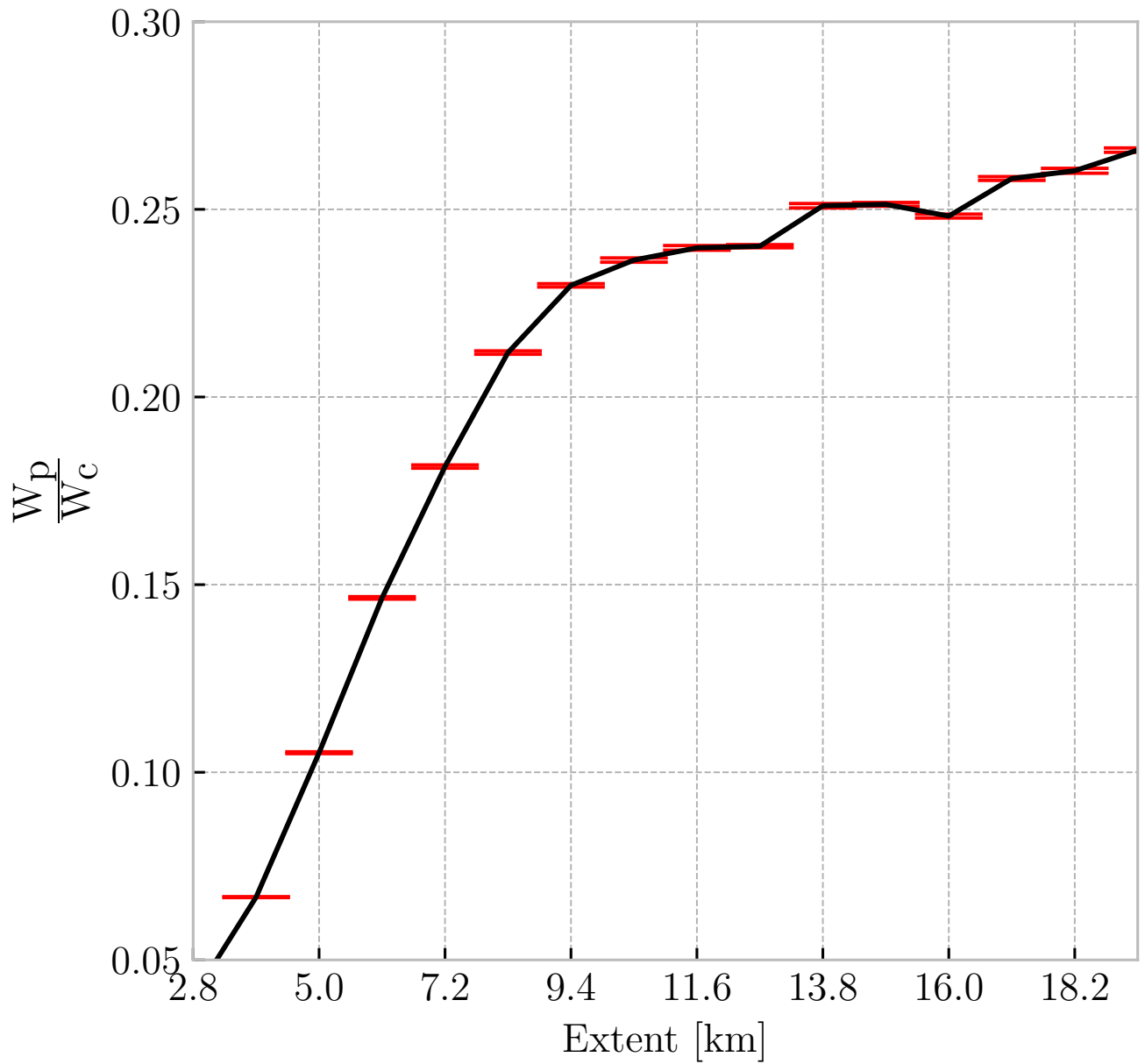


**Figure 2.** The median warm-ratio of cloud water to rain efficiency-water ( $\frac{W_p}{W_c}$ ) at a given median-maximum size (extent). The red errorbars represent ±1 standard deviation of a bootstrapped distribution of ( $\frac{W_p}{W_c}$ ) medians at a given extent.

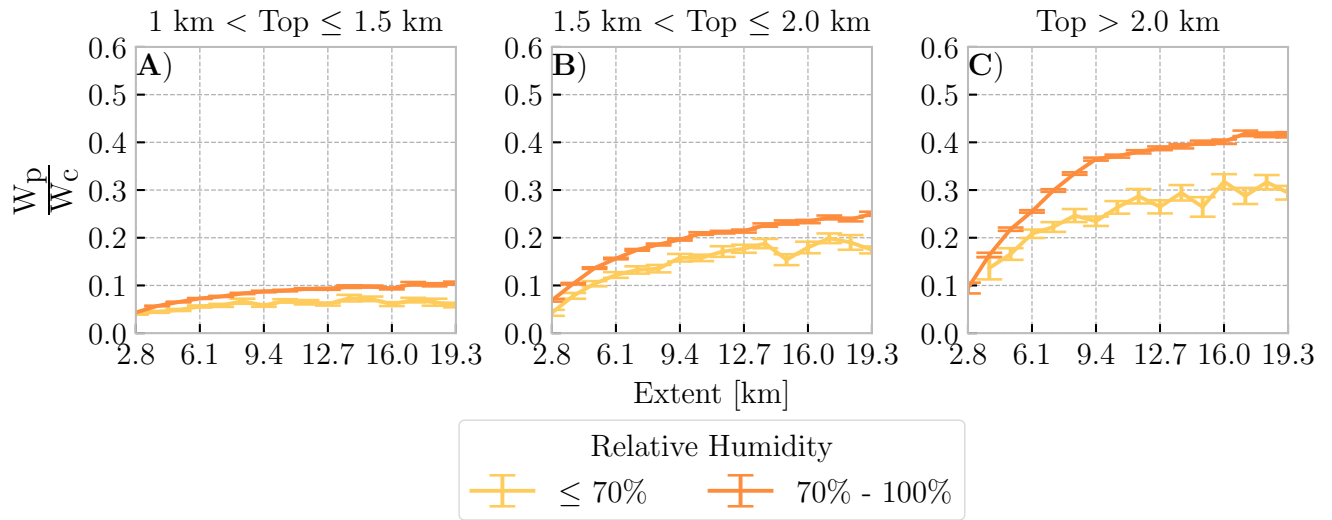


**Figure 3.** The median warm-ratio of cloud water to rain efficiency-water ( $\frac{W_p}{W_c}$ ) at a given median-maximum size (extent). The different line colors represent cloud objects separated by environmental-moisture ( $< 3 \text{ km } 850\text{-mb}$  relative humidity (RH)). Errorbars represent  $\pm 1$  standard deviation of a bootstrapped distribution of  $(\frac{W_p}{W_c})$  medians at a given extent and RH.

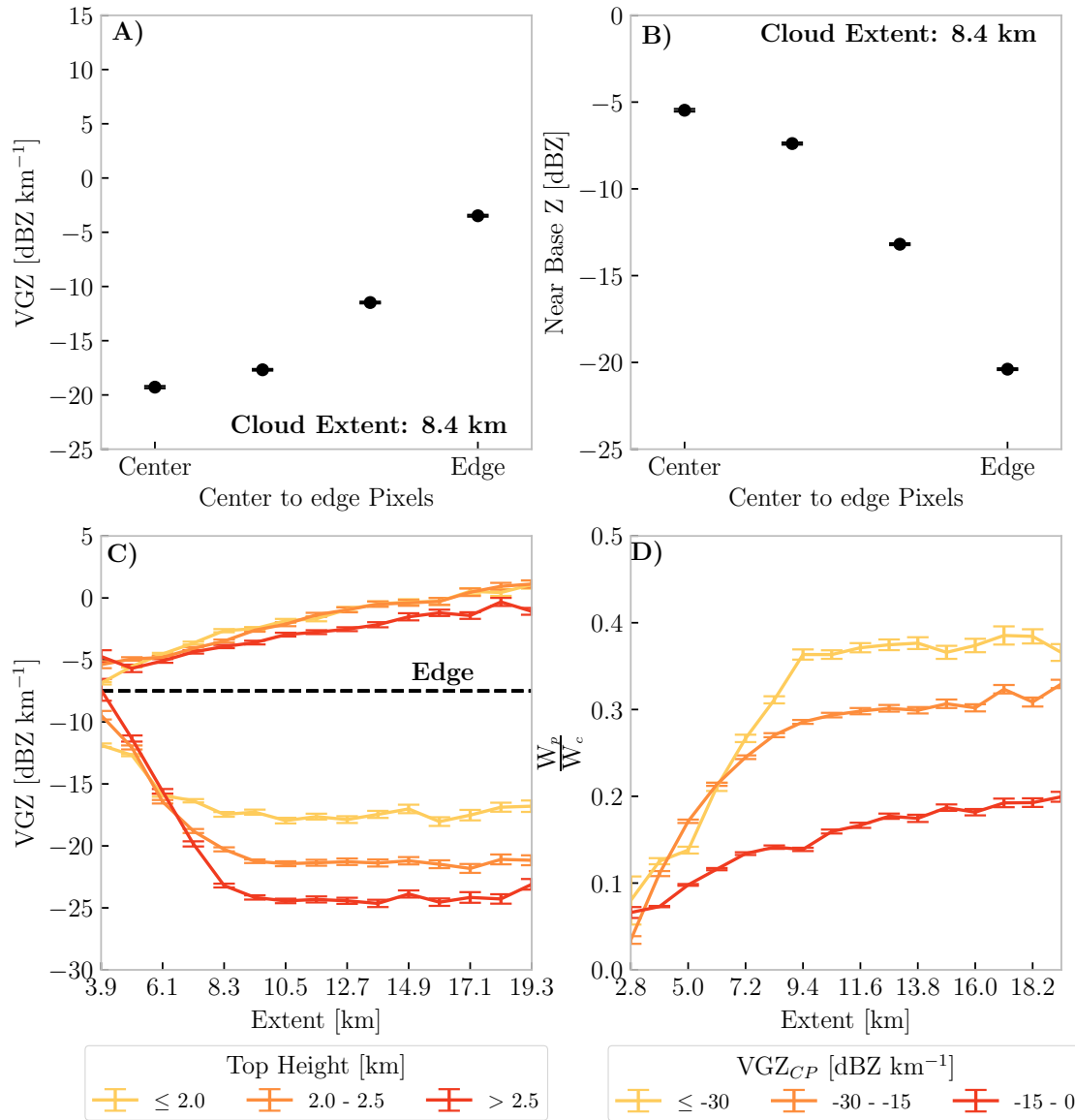


**Figure 4.** Panel A) shows the median change in the vertical reflectivity (VGZ) from the center to edge of all cloud objects with an extent of 10.5–8.4 km. Panel B) shows the median change in near base reflectivity (Z) from the center to edge of all cloud objects with an extent of 8.4 km. Panel C) shows the median vertical reflectivity gradient (VGZ) at the center (red) and edge (blue) of different sized (extent) raining cloud objects. Different lines represent cloud objects separated by top height. Panel D) shows the median warm-ratio of cloud water to rain efficiency-water ( $\frac{W_p}{W_c}$ ) at a given median size (extent). The different line colors represent cloud objects separated by the vertical reflectivity gradient on the center pixel (VGZ<sub>cp</sub>) of all cloud objects. Error bars represent  $\pm 1$  standard deviation of a bootstrapped distribution of median VGZ and Z for a given pixel from cloud object edge to center (Panels A) and B), as well as VGZ and  $\frac{W_p}{W_c}$  at a given extent (Panels C) and D)).

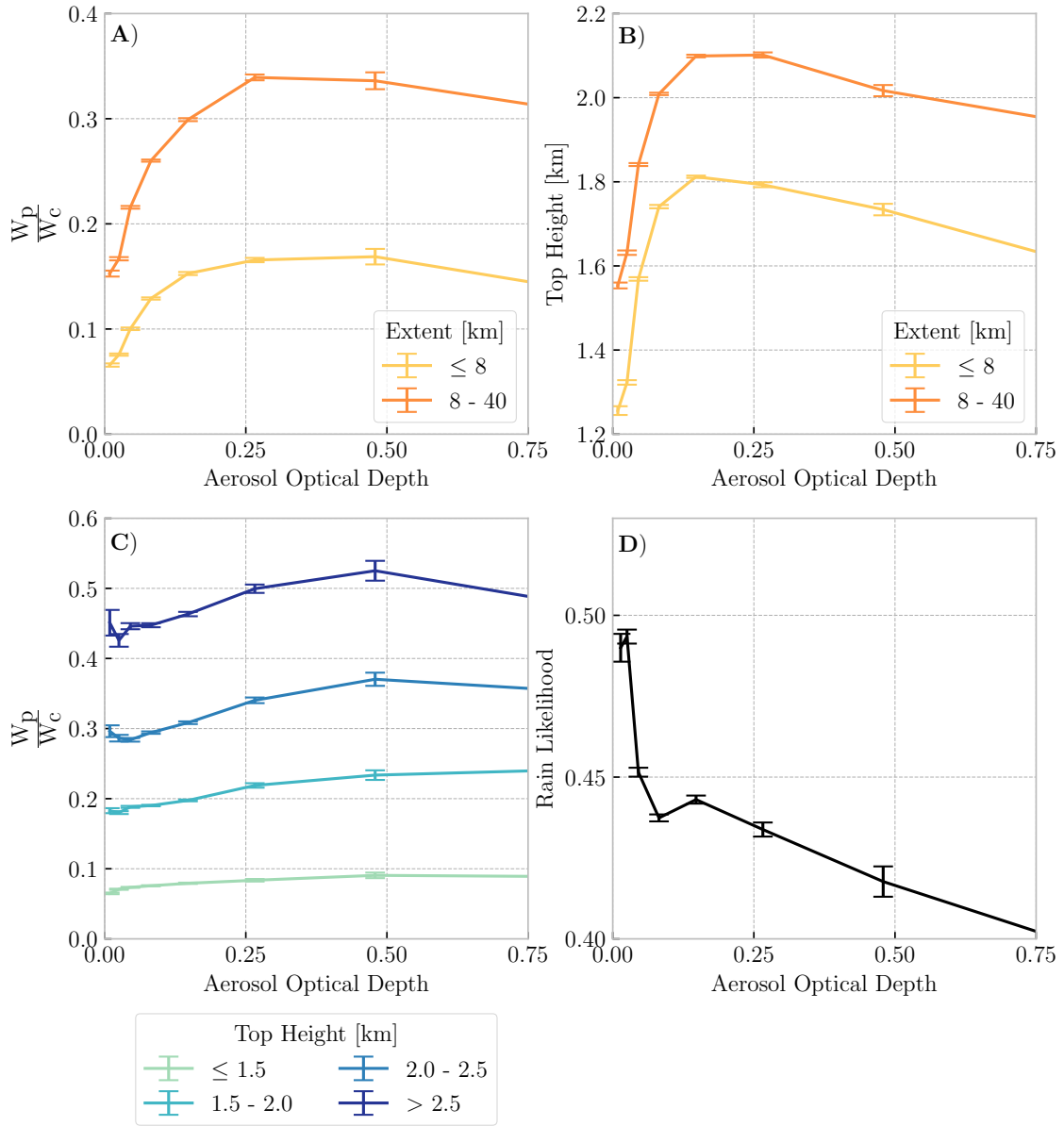


**Figure 5.** Panel A) shows the relationship between median warm rain efficiency as MODIS 550 nm aerosol optical depth. Panel B) shows the relationship between median cloud-top height and aerosol optical depth. Panel C) shows the relationship between warm rain efficiency ( $\frac{W_p}{W_c}$ ) and aerosol optical depth. Line colors in panels A) and B) represent cloud objects separated by extent, while line colors in panel C) represent cloud objects separated by top height. Panel D) shows the ratio of raining cloud objects to non-raining cloud objects (rain likelihood) at a given aerosol optical depth. For panels A), B), and C), errorbars represent  $\pm 1$  standard deviation of a bootstrapped distribution of raining cloud objects to determine the uncertainty in  $\frac{W_p}{W_c}$ , and top height at a given aerosol optical depth. Whereas, the errorbars shown in panel D) represent  $\pm 1$  standard deviation of a bootstrapped distribution of raining and non-raining cloud objects to determine rain likelihood uncertainty at a given aerosol optical depth.

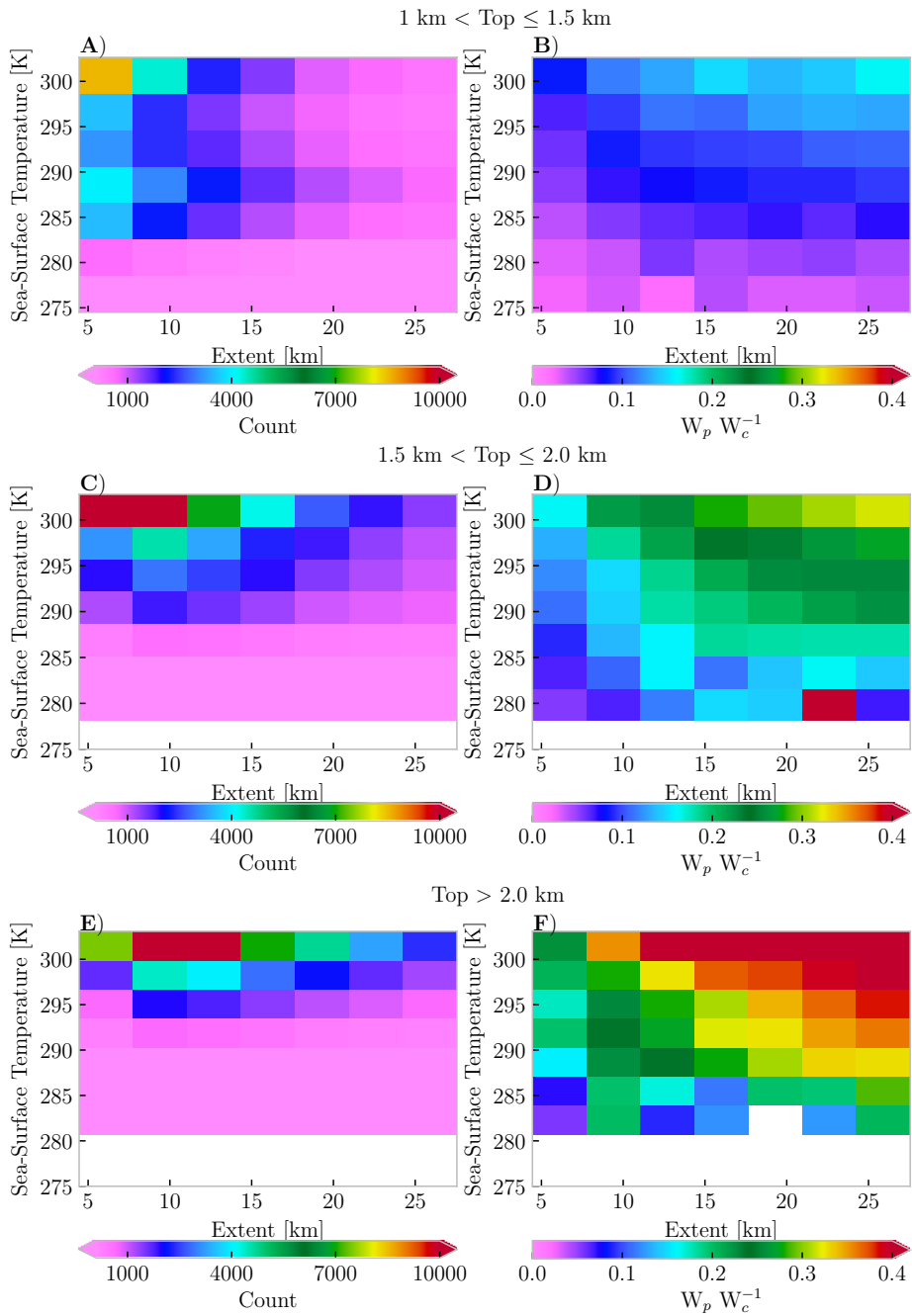


**Figure 6.** The two-dimensional distribution of extent as a function of sea-surface temperature, conditioned by cloud-top height, is shown in panels A), C), and E) respectively. The median warm-ratio of cloud water to rain efficiency-water ( $W_p W_c^{-1}$ ) as a function of Extent and sea-surface temperature are shown in panels B), D), and F) respectively.